isvr Institute of Sound and Vibration Research

Pavement Analysis Part II: SH - Waves

W.H. Coghill

ISVR Technical Memorandum 849

November 1999

University of Southampton

SCIENTIFIC PUBLICATIONS BY THE ISVR

Technical Reports are published to promote timely dissemination of research results by ISVR personnel. This medium permits more detailed presentation than is usually acceptable for scientific journals. Responsibility for both the content and any opinions expressed rests entirely with the author(s).

Technical Memoranda are produced to enable the early or preliminary release of information by ISVR personnel where such release is deemed to the appropriate. Information contained in these memoranda may be incomplete, or form part of a continuing programme; this should be borne in mind when using or quoting from these documents.

Contract Reports are produced to record the results of scientific work carried out for sponsors, under contract. The ISVR treats these reports as confidential to sponsors and does not make them available for general circulation. Individual sponsors may, however, authorize subsequent release of the material.

UNIVERSITY OF SOUTHAMPTON

INSTITUTE OF SOUND AND VIBRATION RESEARCH

DYNAMICS GROUP

Pavement Analysis
Part II: SH-Waves[1]

by

W.H. Cogill

ISVR Technical Memorandum No. 849

November 1999

Authorized for issue by
Dr. M.J. Brennan
Group Chairman

[1] *Part I of this series is "Single-layered inverse: first order approximation", ISVR Technical Memorandum No. 833, January 1999.*

Contents

List of Tables

List of Figures

Chapter 1

SH-waves

1.1 Introduction

Earthen layered systems are assumed to consist of layers of elastic materials overlying a semi-infinite medium. Horizontally-polarized shear waves (SH-waves) may be applied in order to estimate the interface depths of the structure and the elastic properties of the component media. In this chapter, we consider the response to be expected from a system composed of two layers each having a constant thickness, and resting on an underlying medium which is semi-infinite in extent.

1.2 A system consisting of two layers overlying a semi-infinite medium

Starting Expressions

The system is defined in terms of cylindrical co-ordinates (r, θ, z) having the origin at the free surface and z measured positively downwards. The particle displacements are u and v in the r and θ directions respectively. The stresses are denoted by subscripts e.g. $(p_{\theta\theta})_m$, $m = 1, 2, 3$. The suffix 1 denotes quantities in the upper layer, 2 and 3 those in the lower layer and in the semi-infinite medium respectively.

From Nakano [5], the following expressions for the peak values of the shear stresses and displacements are obtained:[1]

(a) In the surface layer,

$$(p_{zr})_1 = -\mu_1 \frac{s_1}{2} \left(A_1 e^{-s_1 z} - A_1' e^{s_1 z} \right) C(k, r, v, \omega) \tag{1.2}$$

[1]The displacements u and v in the r and θ directions decay with increasing depth. The decay is oscillatory or exponential. The decay constant s may therefore be either purely real or purely imaginary. It is defined by

$$s_n = \sqrt{\frac{\omega^2}{c^2} - \frac{\omega^2}{{\beta_n}^2}} = -is_n' = -i\sqrt{\frac{\omega^2}{{\beta_n}^2} - \frac{\omega^2}{c^2}}; \tag{1.1}$$

where $n = 1, 2, 3$ is the layer index, corresponding with the surface layer, the underlying layer or the semi-infinite medium.

$$(p_{\theta z})_1 = -\mu_1 \frac{s_1}{2} \left(A_1 e^{-s_1 z} - A_1' e^{s_1 z}\right) C'(k,r,v,\omega) \tag{1.3}$$

$$u_1 = \frac{1}{2} \left(A_1 e^{-s_1 z} + A_1' e^{s_1 z}\right) C(k,r,v,\omega) \tag{1.4}$$

$$v_1 = \frac{1}{2} \left(A_1 e^{-s_1 z} + A_1' e^{s_1 z}\right) C'(k,r,v,\omega) \tag{1.5}$$

(b) In the second layer,

$$(p_{zr})_2 = -\mu_2 \frac{s_2}{2} \left(A_2 e^{-s_2 z} - A_2' e^{s_2 z}\right) C(k,r,v,\omega) \tag{1.6}$$

$$(p_{\theta z})_2 = -\mu_2 \frac{s_2}{2} \left(A_2 e^{-s_2 z} - A_2' e^{s_2 z}\right) C'(k,r,v,\omega) \tag{1.7}$$

$$u_2 = \frac{1}{2} \left(A_2 e^{-s_2 z} + A_2' e^{s_2 z}\right) C(k,r,v,\omega) \tag{1.8}$$

$$v_2 = \frac{1}{2} \left(A_2 e^{-s_2 z} + A_2' e^{s_2 z}\right) C'(k,r,v,\omega) \tag{1.9}$$

(c) In the semi-infinite medium, we take s_3 to be positive in order that the displacements may vanish as the value of z tends to infinity,

$$(p_{zr})_3 = -\mu_3 \frac{s_3}{2} \left(A_3 e^{-s_3 z}\right) C(k,r,v,\omega) \tag{1.10}$$

$$(p_{\theta z})_3 = -\mu_3 \frac{s_3}{2} \left(A_3 e^{-s_3 z}\right) C'(k,r,v,\omega) \tag{1.11}$$

$$u_3 = \frac{1}{2} \left(A_3 e^{-s_3 z}\right) C(k,r,v,\omega) \tag{1.12}$$

$$v_3 = \frac{1}{2} \left(A_3 e^{-s_3 z}\right) C'(k,r,v,\omega) \tag{1.13}$$

In writing equations (1.10) to (1.13) one boundary condition, that of zero displacement at infinite depth, has already been taken into account. The arbitrary constants A_1, A_1', A_2, A_2' and A_3 can be eliminated using the conditions at the interfaces within the system. The boundary condition at the free surface, namely that the shear stresses are zero in the r, θ plane, is not required.

At the first interface, the stresses and displacements are continuous, i.e. when $z = f$

$$\begin{aligned} u_1 &= u_2, & v_1 &= v_2, \\ (p_{zr})_1 &= (p_{zr})_2, & (p_{\theta z})_1 &= (p_{\theta z})_2 \end{aligned} \tag{1.14}$$

At the second interface, the stresses and displacements are continuous, i.e. when $z = f + g$

$$\begin{aligned} u_2 &= u_3, & v_2 &= v_3, \\ (p_{zr})_2 &= (p_{zr})_3, & (p_{\theta z})_2 &= (p_{\theta z})_3 \end{aligned} \tag{1.15}$$

Owing to similarities between equations (1.2) to (1.5) and (1.6) to (1.9), the conditions relating to displacement and shear stress lead to only one equation.

The use of the boundary conditions (1.14), with equations (1.2) to (1.5) and (1.6) to (1.9), leads to the following equations:

$$A_1e^{-s_1f} + A_1'e^{s_1f} = A_2e^{-s_2f} + A_2'e^{s_2f} \quad (1.16)$$

$$\text{and } \mu_1 s_1 A_1e^{-s_1f} - A_1'e^{s_1f} = \mu_2 s_2 A_2e^{-s_2f} - A_2'e^{s_2f} \quad (1.17)$$

The use of the boundary conditions (1.15) with equations (1.6) to (1.9) and (1.10) to (1.13), leads to the following equations:

$$A_2e^{-s_2(f+g)} + A_2'e^{s_2(f+g)} = A_3e^{-s_3(f+g)} \quad (1.18)$$

$$\text{and } \mu_2 s_2 A_2e^{-s_2(f+g)} - A_2'e^{s_2(f+g)} = \mu_3 s_3 A_3e^{-s_3(f+g)} \quad (1.19)$$

The constant A_3 must be non-zero, to account for finite displacements in the underlying medium. Therefore A_1, A_1', A_2, A_2' and A_3 can be eliminated from equations (1.16) , (1.17), (1.18) and (1.19), and the following wave velocity equation is obtained [7]:-

$$\begin{aligned}(\mu_3 s_3 coshs_2g &+\mu_2 s_2 sinhs_2g)\mu_2 s_2 coshs_1f \\ + \ &(\mu_3 s_3 sinhs_2g + \mu_2 s_2 coshs_2g)\mu_1 s_1 sinhs_1f = 0\end{aligned} \quad (1.20)$$

Several forms of equation (1.20) are possible. These depend on whether the displacements are considered to vary exponentially or in an oscillatory manner with the depth. Equation (1.20) yields no solution if s_1, s_2 and s_3 are all considered imaginary. Therefore oscillatory variation in all three media cannot occur.

1.3 Forms of Equation (1.20)

Four forms of equation (1.20) are considered.

(i)	s_1	imaginary,	s_2	real	(Case 1)
(ii)	s_1	real,	s_2	imaginary	(Case 2)
(iii)	s_1, s_2		both imaginary		(Case 3)
(iv)	s_1, s_2		both real		(Case 4)

cases14

1.3.1 Case 1

Write $s_1 = i\bar{s}_1$. From equation (1.20) there is obtained

$$tan\ \bar{s_1}f = \frac{\mu_2 s_2}{\mu_1 \bar{s_1}} . \frac{\mu_3 s_3\ cosh\ s_2g + \mu_2 s_2\ sinh\ s_2g}{\mu_3 s_3\ sinh\ s_2g + \mu_2 s_2\ cosh\ s_2g} \quad (1.21)$$

Put $\frac{\mu_3 s_3}{\mu_2 s_2} = tanh\ \psi$, then $tan\ \bar{s}_1 f = \frac{\mu_2 s_2}{\mu_1 \bar{s}_1}\ tanh\ (s_2g + \psi)$.
On writing $\bar{s}_1, s_2$ and s_3 in full and re-arranging, there is obtained

$$\lambda = \frac{2\pi f\sqrt{\frac{c^2}{\beta^2{}_1} - 1}}{tan^{-1}\left\{\frac{\mu_2\beta_1}{\mu_1\beta_2}\sqrt{\frac{\beta_2{}^2 - c^2}{c^2 - \beta_1{}^2}}.tanh(\frac{2\pi g}{\lambda}\sqrt{1 - \frac{c^2}{\beta^2{}_2}} + \psi)\right\}} \quad (1.22)$$

1.3.2 Case 2

Write $s_2 = i\bar{s}_2$. From equation (1.20) there is obtained

$$tanh\ s_1 f = \frac{\mu_2 \bar{s}_2}{\mu_1 s_1} . \frac{-\mu_3 s_3\ cos\ \bar{s}_2 g + \mu_2 \bar{s}_2\ sin\ \bar{s}_2 g}{\mu_3 s_3\ sin\ \bar{s}_2 g + \mu_2 s_2\ cos\ \bar{s}_2 g} . \tag{1.23}$$

Put $\frac{\mu_3 s_3}{\mu_2 \bar{s}_2} = tan\ \psi$, then $tanh\ s_1 f = \frac{\mu_2 \bar{s}_2}{\mu_1 s_1}\ tan\ (\bar{s}_2 g - \psi)$.
On writing $s_1, \bar{s}_2$ and s_3 in full and re-arranging, there is obtained

$$\lambda = \frac{2\pi f \sqrt{1 - \frac{c^2}{{\beta_1}^2}}}{tanh^{-1}\left\{ \frac{\mu_2 \beta_1}{\mu_1 \beta_2} \sqrt{\frac{c^2 - {\beta_2}^2}{{\beta_1}^2 - c^2}}\ tan(\frac{2\pi g}{\lambda} \sqrt{\frac{c^2}{\beta^2{}_2} - 1} - \psi) \right\}} \tag{1.24}$$

1.3.3 Case 3

Write $s_1 = i\bar{s}_1, s_2 = i\bar{s}_2$. From equation (1.20) there is obtained

$$tan\ \bar{s}_1 f = \frac{\mu_2 \bar{s}_2}{\mu_1 \bar{s}_1} . \frac{\mu_3 s_3\ cos\ \bar{s}_2 g - \mu_2 \bar{s}_2\ sin\ \bar{s}_2 g}{\mu_3 s_3\ sin\ \bar{s}_2 g + \mu_2 \bar{s}_2\ cos\ \bar{s}_2 g} . \tag{1.25}$$

Put $\frac{\mu_3 s_3}{\mu_2 s_2} = cot\ \psi$, then $tan\ \bar{s}_1 f = \frac{\mu_2 \bar{s}_2}{\mu_1 \bar{s}_1}\ cot\ (\bar{s}_2 g + \psi)$.
On writing $\bar{s}_1, \bar{s}_2$ and s_3 in full and re-arranging, there is obtained

$$\lambda = \frac{2\pi f \sqrt{\frac{c^2}{{\beta_1}^2} - 1}}{tan^{-1}\left\{ \frac{\mu_2 \beta_1}{\mu_1 \beta_2} \sqrt{\frac{c^2 - {\beta_2}^2}{c^2 - {\beta_1}^2}}\ cot(\frac{2\pi g}{\lambda} \sqrt{\frac{c^2}{{\beta_2}^2} - 1} + \psi) \right\}} \tag{1.26}$$

1.3.4 Case 4

From equation (1.20) there is obtained

$$tanh\ s_1 f = -\frac{\mu_2 s_2}{\mu_1 s_1} . \frac{\mu_3 s_3\ cosh\ s_2 g + \mu_2 s_2\ sinh\ s_2 g}{\mu_3 s_3\ sinh\ s_2 g + \mu_2 s_2\ cosh\ s_2 g} . \tag{1.27}$$

Put $\frac{\mu_3 s_3}{\mu_2 s_2} = coth\ \psi$, then $tanh\ s_1 f = -\frac{\mu_2 s_2}{\mu_1 s_1}\ coth\ (s_2 g + \psi)$.
On writing s_1, s_2 and s_3 in full and re-arranging, there is obtained

$$\lambda = -\frac{2\pi f \sqrt{\frac{c^2}{{\beta_1}^2} - 1}}{tanh^{-1}\left\{ \frac{\mu_2 \beta_1}{\mu_1 \beta_2} \sqrt{\frac{{\beta_2}^2 - c^2}{{\beta_1}^2 - c^2}}\ coth(\frac{2\pi g}{\lambda} \sqrt{1 - \frac{c^2}{{\beta_2}^2}} + \psi) \right\}} \tag{1.28}$$

1.4 Matrix Methods

Most systems which are of practical importance are more complex that those considered in the first part of this chapter. The systems comprise several layers. The layers may be interspersed in any order of stiffness. The deepest layer of which the system is composed is usually regarded as extending to infinite depth, and is represented by a semi-infinite medium. A method is required of calculating the phase velocities of SH waves at the free surfaces of these structures. It is expected that the phase velocities will vary with the frequency. The phase velocities will be complex quantities if leaking modes are considered (Su and Dorman, [10]).

The method proposed by Thomson[11] will be followed, and use will made of the notation employed by Thrower[12]. The component materials are considered as purely elastic, and leaking modes are not considered. The vector representing the shear stress $p_{\theta z}$ and the displacement v in the m-th medium from the free surface can be written

$$\bar{W}_m = (p_{\theta z}, v) \tag{1.29}$$

The peak value of the shear stress can be written (Nakano, [5])

$$\begin{aligned} p_{\theta z} &= -\frac{\mu s}{2}(Ae^{-sz} - A'e^{sz}).C'(k,r,v,w) && (1.30)\\ &= \frac{\mu s}{2}(S\ sinh\ sz + S'\ cosh\ sz).C'(k,r,v,w), && (1.31) \end{aligned}$$

where $S = A' + A$ and $S' = A' - A$, and the peak value of the displacement can be written

$$\begin{aligned} v &= \frac{1}{2}(Ae^{-sz} + A'e^{sz}).C'(k,r,v,w) && (1.32)\\ &= \frac{1}{2}(S\ cosh\ sz + S'\ sinh\ sz).C'(k,r,v,w). && (1.33) \end{aligned}$$

Here C' is some circular function, the exact form of which is not important as it cancels when the boundary conditions are applied. As the trajectory of the particle motion is horizontal and purely tangential to the direction of propagation, only one shear stress and one displacement need be considered. This suffices to determine the stresses and displacements throughout the system.

In matrix notation

$$\bar{W}_m = \bar{Q}_m.\bar{B}_m \tag{1.34}$$

where

$$\bar{B}_m = \begin{bmatrix} S \\ S' \end{bmatrix} \text{ and} \tag{1.35}$$

$$\bar{Q}_m = \begin{pmatrix} \frac{\mu s}{2}\ sinh\ sz & \frac{\mu s}{2} cosh\ sz \\ \frac{1}{2}\ cosh\ sz & \frac{1}{2}\ sinh\ sz \end{pmatrix}_m \tag{1.36}$$

where the suffix m denotes that the quantities are those whch apply to the m-th medium below the free surface of the structure. Placing the origin of the co-ordinates at the $(m-1)$-th interface, the expression for the stress-displacement vector $\bar{W}_{m,m-1}$, within the m-th layer at the $(m-1)$-th interface is

$$\bar{W}_{m,m-1} = \bar{C}_m.\bar{B}_m, \quad \begin{matrix} \bar{B} \text{ is 2(row) x 1 (column)} \\ \bar{C} \text{ is 2(row) x 2 (column)} \\ \bar{W} \text{ is 2(row) x 1 (column)} \end{matrix} \tag{1.37}$$

where $\bar{C}_m$ is derived from $\bar{Q}_m$ by putting $z = 0$. The stress-displacement vector $\bar{W}_{m,m}$ within the m-th layer at the m-th interface is

$$\bar{W}_{m,m} = \bar{D}_m.\bar{B}_m, \quad \bar{D} \text{ is 2(row) x 2 (column)} \tag{1.38}$$

where $\bar{D}_m$ is derived from $\bar{Q}_m$ by putting $z = H_m$, the thickness of the $m-$th layer. Equation (1.37) can be written

$$\bar{B}_m = \bar{C}_m^{-1}\bar{W}_{m,m-1}, \quad \bar{C}_m^{-1} \text{ is 2(row) x 2 (column)} \tag{1.39}$$

The vectors $\bar{W}_{m,m-1}$ and $\bar{W}_{m,m}$, representing the stresses and displacements at the top and bottom of the $m-$th layer, are therefore related by

$$\bar{W}_{m,m} = \bar{D}_m\bar{C}_m^{-1}\bar{W}_{m,m-1}. \quad \bar{D}\bar{C}^{-1} \text{ is 2(row) x 2 (column)} \tag{1.40}$$

It is assumed that there is no slip at the interface[12]; the stress-displacement vectors on either side of the interface must be equal, or

$$\bar{W}_{m,m-1} = \bar{W}_{m-1,m-1}. \tag{1.41}$$

Equation (1.40) can be written as

$$\bar{W}_{m,m} = \bar{D}_m\, \bar{C}_m^{-1}\, \bar{W}_{m-1,m-1}. \tag{1.42}$$

Writing $\bar{C}_m^{-1} = \bar{E}_m$, $\bar{E}$ is 2(row) x 2(column), the previous equation can be applied to each interface in turn, starting with the lowest interface, the n-th. This yields,

$$\begin{matrix} \bar{W}_{n,n} & = \bar{E}_n\, \bar{E}_{n-1}...\bar{E}_1\, \bar{W}_{1,0} & \\ & = \bar{F}\, \bar{W}_{1,0}, & \bar{F} \text{ is 2(row) x 2 (column)} \end{matrix} \tag{1.43}$$

If the semi-infinite medium is absent, the problem is that of a layered free plate. The boundary conditions on each of the free surfaces require that $p_{\theta z} = 0$. Therefore[2]

$$f_{12} = 0 \tag{1.44}$$

This is the equation relating the phase velocity at the free surface, c to the wavelength λ.

[2]In the case of a free plate, $\bar{W}_{1,0} = (0, v)$, where the zero represents the shear stress and the v represents some finite displacement. Similarly, $\bar{W}_{n,n} = (0, v)$. On writing the matrices in full it will be seen that both these conditions can be satisfied on if f_{12} is zero.

If the semi-infinite medium, designated by the sequential number $(n+1)$, is present, the problem is that of a layered half space. Pre-multiplying (1.43) by $\bar{C}_{n+1}^{-1}$ yields

$$\bar{B}_{n+1} = \bar{C}_{n+1}^{-1} \bar{F}\, \bar{W}_{1,0} = \bar{J}\, \bar{W}_{1,0}, \bar{J} \text{ is 2(row) x 2 (column);} \tag{1.45}$$

The condition in the semi-infinite medium is that there are no sources at infinite depth. This implies that $S_{n+1} = -S'_{n+1}$. At the free surface, the shear stress is zero but the displacement is non-zero. This condition can only be satisfied if

$$j_{12} + j_{22} = 0 \tag{1.46}$$

Equation (1.46) is the frequency equation of the system. It contains the phase velocity and the wavelength implicitly as a function of the shear elastic moduli and of the velocities of propagation of shear waves in the media composing the system. The thicknesses of the layers of the component materials are required, and are assumed to be constants.

1.5 Checks of matrix methods.

The results obtained lead to equations relating the phase velocity at the free surface to the frequency or to the wavelength. These equations can be checked by comparing the results with known solutions. Solutions are available for some specific types of structure.

In order to obtain the frequency equation of the system, it is necessary to write in full the $\bar{C}, \bar{C}^{-1}, \bar{D}$ and $\bar{E}$ matrices. The $\bar{C}$ matrix is obtained from the $\bar{Q}$ matrix, by putting $z = 0$, and is

$$\bar{C} = \begin{vmatrix} 0 & \frac{\mu s}{2} \\ \frac{1}{2} & 0 \end{vmatrix}. \tag{1.47}$$

It can be verified that

$$\bar{C}^{-1} = \begin{vmatrix} 0 & 2 \\ \frac{2}{\mu s} & 0 \end{vmatrix}. \tag{1.48}$$

The $\bar{D}$ matrix is derived from the $\bar{Q}$ matrix, putting $z = H$, and is

$$\bar{D} = \begin{vmatrix} \frac{\mu s}{2} \sinh sH & \frac{\mu s}{2} \cosh sH \\ \frac{1}{2} \cosh sH & \frac{1}{2} \sinh sH; \end{vmatrix}. \tag{1.49}$$

finally, $\bar{E} = \bar{D}\, \bar{C}^{-1}$, and is given by

$$\bar{D} = \begin{vmatrix} \cosh sH & \mu s \sinh sH \\ \frac{1}{\mu s} \sinh sH & \cosh sH \end{vmatrix}. \quad (1.50)$$

The matrices denoted by $\bar{C}$, $\bar{D}$ and $\bar{F}$ were obtained for plane waves by Haskell[2].

(i) Consider a two-layered free plate. The matrix $\bar{F}$, defined in equation (1.43), is given by

$$F = E_1 E_2 = \begin{vmatrix} \cosh s_2 g & \mu_2 s_2 \sinh s_2 g \\ \frac{1}{\mu_2 s_2} \sinh s_2 g & \cosh s_2 g \end{vmatrix} \cdot \begin{vmatrix} \cosh s_1 f & \mu_1 s_1 \sinh s_1 f \\ \frac{1}{\mu_1 s_1} \sinh s_1 f & \cosh s_1 f \end{vmatrix} \quad (1.51)$$

The frequency equation of the system can be obtained as shown previously (1.44), and is given by

$$f_{12} = \mu_1 s_1 \sinh s_1 f \cosh s_2 g + \mu_2 s_2 \sinh s_2 g \cosh s_1 f = 0. \quad (1.52)$$

As shown by Kurzeme [3], equation (1.52) is identical with that obtained by considering the constructive interference of waves in this system (Officer [6]; Tolstoy and Usdin [13]).

(ii) Consider next the case of a single layer of constant thickness overlying a semi-infinite medium. If the layer is composed of a material having a lower stiffness than that of the material composing the semi-infinite medium, the system is the same as that treated by Love [4], for which the frequency equation is known(Nakano, [5]). The elements j_{12} and j_{22} are required, and can be obtained as follows:

$$\bar{J} = \bar{C}_2^{-1}\bar{F} = \bar{C}_2^{-1}\bar{E}_1 = \begin{vmatrix} 0 & 2 \\ \frac{2}{\mu_2 s_2} & 0 \end{vmatrix} \cdot \begin{vmatrix} \cosh s_1 f & \mu_1 s_1 \sinh s_1 f \\ \frac{1}{\mu_1 s_1} \sinh s_1 f & \cosh s_1 f \end{vmatrix} \quad (1.53)$$

$$\bar{J} = \bar{C}_2^{-1}\bar{F} = \bar{C}_2^{-1}\bar{E}_1 \quad (1.54)$$

$$= \begin{vmatrix} 0 & 2 \\ \frac{2}{\mu_2 s_2} & 0 \end{vmatrix} \cdot \begin{vmatrix} \cosh s_1 f & \mu_1 s_1 \sinh s_1 f \\ \frac{1}{\mu_1 s_1} \sinh s_1 f & \cosh s_1 f \end{vmatrix} \quad (1.55)$$

$$= \begin{vmatrix} \frac{2}{\mu_1 s_1} \sinh s_1 f & 2 \cosh s_1 f \\ \frac{2}{\mu_2 s_2} \cosh s_1 f & 2 \frac{\mu_1 s_1}{\mu_2 s_2} \sinh s_1 f \end{vmatrix} \quad (1.56)$$

The equation relating the wavelength and the phase velocity is

$$j_{12} + j_{22} = 0 \tag{1.57}$$

$$\text{i.e. } \frac{\mu_1 s_1}{\mu_2 s_2} \sinh s_1 f + \cosh s_1 f = = 0 \tag{1.58}$$

Equation (1.58) is not directly comparable with known solutions. If $c^2 > {\beta_1}^2$,

$$s_1 = \sqrt{\frac{\omega^2}{c^2} - \frac{\omega^2}{{\beta_1}^2}} = -is_1' = -i\sqrt{\frac{\omega^2}{{\beta_1}^2} - \frac{\omega^2}{c^2}}; \tag{1.59}$$

also $\cosh iy = \cos(-y)$ and $\sinh iy = i \sin y$ where y is any quantity.

Equation (1.58) becomes

$$\frac{\mu_1(is_1)}{\mu_2 s_2} \sinh(-is_1' f) + \cosh(-is_1' f) = 0$$

$$\text{i.e. } \frac{\mu_1(-is_1)}{\mu_2 s_2} i \sin(-s_1' f) + \cos(s_1' f) = 0$$

$$\text{therefore } -\frac{\mu_1 s_1'}{\mu_2 s_2} \sin(s_1' f) + \cos(s_1' f) = 0$$

$$\text{or } \tan s_1' f = \frac{\mu_2 s_2}{\mu_1 s_1'}$$

in agreement with known results [4] [1]. (iii) Finally, consider a system consisting of two layers overlying a semi-infinite medium. The elements of $\bar{F}$ can be found from the expression used to derive (1.52) and are as follows:-

$$f_{11} = \cosh s_1 f \cosh s_2 g + \frac{\mu_2 s_2}{\mu_1 s_1} \sinh s_1 f \sinh s_2 g, \tag{1.60}$$

$$f_{12} = \mu_1 s_1 \sinh s_1 f \cosh s_2 g + \mu_2 s_2 \cosh s_1 f \sinh s_2 g, \tag{1.61}$$

$$f_{21} = \frac{1}{\mu_2 s_2} \cosh s_1 f \sinh s_2 g + \frac{1}{\mu_1 s_1} \sinh s_1 f \cosh s_2 g \tag{1.62}$$

$$\text{and } f_{22} = \frac{\mu_1 s_1}{\mu_2 s_2} \sinh s_1 f \sinh s_2 g + \mu_2 s_2 \cosh s_1 f \cosh s_2 g. \tag{1.63}$$

If $\bar{F}$ is pre-multiplied by $\bar{C}_3^{-1}$, and retaining only the significant elements, the following is obtained:

$$j_{12} = 2\left(\frac{\mu_1 s_1}{\mu_2 s_2} \sinh s_1 f \sinh s_2 g + \mu_2 s_2 \cosh s_1 f \cosh s_2 g\right) \tag{1.64}$$

$$j_{22} = \frac{2}{\mu_3 s_3} (\mu_1 s_1 \sinh s_1 f \cosh s_2 g + \mu_2 s_2 \cosh s_1 f \sinh s_2 g). \tag{1.65}$$

The equation relating the wavelength and the phase velocity is

$$j_{12} + j_{22} = 0 \tag{1.66}$$

If the expressions for j_{12} and j_{22} are substituted in (1.66), the frequency equation can be written as follows:

$$2\left(\frac{\mu_1 s_1}{\mu_2 s_2}\, sinh\, s_1 f\, sinh\, s_2 g \;+\; \mu_2 s_2\, cosh\, s_1 f\, cosh\, s_2 g\right) +$$
$$\frac{2}{\mu_3 s_3}\,(\mu_1 s_1\, sinh\, s_1 f\, cosh\, s_2 g \;+\; \mu_2 s_2\, cosh\, s_1 f\, sinh\, s_2 g) = 0. \qquad (1.67)$$

This equation can be simplified as follows:

$$\mu_3 s_3\,(\mu_1 s_1\, sinh\, s_1 f\, sinh\, s_2 g \;+\; \mu_2 s_2\, cosh\, s_1 f\, cosh\, s_2 g) +$$
$$\mu_2 s_2\,(\mu_1 s_1\, sinh\, s_1 f\, cosh\, s_2 g \;+\; \mu_2 s_2\, cosh\, s_1 f\, sinh\, s_2 g) = 0. \qquad (1.68)$$

or,

$$(\mu_3 s_3\, cosh\, s_2 g \;+\; \mu_2 s_2\, sinh\, s_2 g)\,\mu_2 s_2\, cosh\, s_1 f +$$
$$(\mu_3 s_3\, sinh\, s_2 g \;+\; \mu_2 s_2\, cosh\, s_2 g)\,\mu_1 s_1\, sinh\, s_1 f \;=\; 0. \qquad (1.69)$$

This is identical with equation (1.20). It is the frequency equation of the system, and can be satisfied by pairs of values of the phase velocity and the frequency.

1.6 Discussion of equations (1.22) to (1.28)

Discussion

The propagation of horizontally-polarized shear waves (Love waves) has been comprehensively studied([4], [8], [5]). The structure analysed by Love [4] consists of a single solid layer of finite thickness overlying a semi-infinite medium. An oscillatory torque is applied to the free surface of the structure, in order to generate horizontally-polarized shear waves in the structure. The phase velocity of the waves is measured at the free surface of the structure. The phase velocity is not a constant, but varies with the wavelength of the oscillation. The response of a two-layered system is similar but contains additional branches, represented by equations (1.22) to (1.28). It is sometimes convenient to present experimental data graphically. There are advantages in considering the relationships between the phase velocity at the free surface and the angular frequency of the waves propagated. Equations (1.22) to (1.28) may be expressed in the following alternate form.

Case 1

$$\lambda = \frac{2\pi f\sqrt{\dfrac{c^2}{{\beta^2}_1} - 1}}{tan^{-1}\left\{\dfrac{\mu_2\beta_1}{\mu_1\beta_2}\sqrt{\dfrac{{\beta_2}^2 - c^2}{c^2 - {\beta_1}^2}}.tanh(\dfrac{\omega g}{\beta_2}\sqrt{\dfrac{{\beta_2}^2}{c^2} - 1 + \psi})\right\}} \qquad (1.70)$$

$$tan\frac{\omega f}{\beta_1}\sqrt{1 - \frac{{\beta_1}^2}{c^2}} = \frac{\mu_2\beta_1}{\mu_1\beta_2}\sqrt{\frac{{\beta_2}^2 - c^2}{c^2 - {\beta_1}^2}}.tanh\left(\frac{\omega g}{\beta_2}\sqrt{\frac{{\beta_2}^2}{c^2} - 1 + \psi}\right) \qquad (1.71)$$

where

$$tanh\,\psi = \frac{\mu_3\beta_2}{\mu_2\beta_3}\sqrt{\frac{{\beta_3}^2 - c^2}{{\beta_2}^2 - c^2}}. \qquad (1.72)$$

Case 2

$$\lambda = \frac{2\pi f\sqrt{1-\frac{c^2}{{\beta_1}^2}}}{tanh^{-1}\left\{\frac{\mu_2\beta_1}{\mu_1\beta_2}\sqrt{\frac{c^2-{\beta_2}^2}{{\beta_1}^2-c^2}}\,tan(\frac{\omega g}{\beta_2}\sqrt{1-\frac{{\beta_2}^2}{c^2}}-\psi)\right\}} \tag{1.73}$$

$$tanh\frac{\omega f}{\beta_1}\sqrt{\frac{{\beta_1}^2}{c^2}-1} = \frac{\mu_2\beta_1}{\mu_1\beta_2}\sqrt{\frac{c^2-{\beta_2}^2}{{\beta_1}^2-c^2}}\,tan\left(\frac{\omega g}{\beta_2}\sqrt{1-\frac{{\beta_2}^2}{c^2}}-\psi\right) \tag{1.74}$$

where

$$tan\,\psi = \frac{\mu_3\beta_2}{\mu_2\beta_3}\sqrt{\frac{{\beta_3}^2-c^2}{c^2-{\beta_2}^2}}. \tag{1.75}$$

Case 3

$$\lambda = \frac{2\pi f\sqrt{\frac{c^2}{{\beta_1}^2}-1}}{tan^{-1}\left\{\frac{\mu_2\beta_1}{\mu_1\beta_2}\sqrt{\frac{c^2-{\beta_2}^2}{c^2-{\beta_1}^2}}\,cot(\frac{\omega g}{\beta_2}\sqrt{1-\frac{{\beta_2}^2}{c^2}}+\psi)\right\}} \tag{1.76}$$

$$tan\frac{\omega f}{\beta_1}\sqrt{1-\frac{{\beta_1}^2}{c^2}} = \frac{\mu_2\beta_1}{\mu_1\beta_2}\sqrt{\frac{c^2-{\beta_2}^2}{c^2-{\beta_1}^2}}\,cot\left(\frac{\omega g}{\beta_2}\sqrt{1-\frac{{\beta_2}^2}{c^2}}+\psi\right) \tag{1.77}$$

where

$$cot\,\psi = \frac{\mu_3\beta_2}{\mu_2\beta_3}\sqrt{\frac{{\beta_3}^2-c^2}{c^2-{\beta_2}^2}}. \tag{1.78}$$

Case 4

$$\lambda = -\frac{2\pi f\sqrt{\frac{c^2}{{\beta_1}^2}-1}}{tanh^{-1}\left\{\frac{\mu_2\beta_1}{\mu_1\beta_2}\sqrt{\frac{{\beta_2}^2-c^2}{{\beta_1}^2-c^2}}\,coth(\frac{\omega g}{\beta_2}\sqrt{\frac{{\beta_2}^2}{c^2}-1}+\psi)\right\}} \tag{1.79}$$

$$tanh\frac{\omega f}{\beta_1}\sqrt{\frac{{\beta_1}^2}{c^2}-1} = \frac{\mu_2\beta_1}{\mu_1\beta_2}\sqrt{\frac{{\beta_2}^2-c^2}{{\beta_1}^2-c^2}}\,coth\left(\frac{\omega g}{\beta_2}\sqrt{\frac{{\beta_2}^2}{c^2}-1}+\psi\right) \tag{1.80}$$

where

$$coth\,\psi = \frac{\mu_3\beta_2}{\mu_2\beta_3}\sqrt{\frac{{\beta_3}^2-c^2}{{\beta_2}^2-c^2}}. \tag{1.81}$$

It is desirable to develop approximate relationships for equations (1.71) to (1.80). These will be discussed in the sections which follow. Approximations

1.7 Approximations to equations (1.71) to (1.80)

The following is the result of a further study of equations (1.71) to (1.80). The expressions do not yield the wavelength explicitly as a function of the wave velocity. Iterative computation is necessary. Nevertheless there are certain values of the independent variable (the phase velocity) at which explicit relations are obtainable. Ths occurs particularly at the terminal velocities and under limiting conditions of the frequencies. Results can then be calculated directly. This is useful for curve tracing, before devoting effort to detailed computations.

The existence of a solution to equation (1.20) indicates that a structure possessing a particular combination of parameters will respond to excitation and yield the indicated relationship between wave-length and phase velocity. The assumptions may, however, involve an over simplification of the physical conditions which exist in the structure.

The prospects of generating a response in any particular branch are a matter of speculation, therefore. Cases 2 and 3 are related to the case of a freely suspended plate, and appear likely to receive confirmation from experiment. If μ_2 and μ_3 are made equal to zero, the expression obtained for Case 3 reduces to the expression governing the propagation of horizontally polarized shear waves in a simple plate(equation (1.58)). Cases 2 and 3 involve trigonometric but not hyperbolic functions. An infinite number of modes of response may therefore be expected, corresponding with successive branches of the functions.

Road pavements are examples of systems composed of dissimilar materials. The relative values of the parameters of the materials are often such that cases 2 and 3 are applicable.

The behaviour of these structures may possibly be represented by the expressions obtained for cases 2 and 3. The cases are considered together because they apply to the same type of structure. Case 3 represents the behaviour if the phase velocity at the free surface exceeds the velocity of shear waves in the upper layer. Case 2 applies if this is not so, and in that case the phase velocity cannot exceed the velocity of shear waves in the underlying medium.

If the underlying medium possesses a stiffness which is negligible in comparison with that of the lower layer, shear waves are multiply reflected from the free surface and the underside of the lower layer. The system behaves as a compound free plate, and the phase velocity at the free surface may become infinite. The theory which applies has been considered by Stoneley [9]. This case constitutes a special one in the present work. It is useful practically, as the predicted large phase velocities are easy to detect, and are characteristic of a particular kind of structure. No solution exists for phase velocities less than the shear wave velocity in the lower layer. Usually, therefore, cases 2 and 3 apply if the phase velocities at the free surface lie between the shear wave velocity in the lower layer and that in the underlying medium.

It is found experimentally that the two surface layers of a pavement or airport runway (media 1 and 2) tend to vibrate as a composite plate. If the shear modulus of rigidity of the underlying medium (medium 3) is assumed to be small compared with that in the lower layer (medium 2) we have, for Case 2 (equation (1.74))

$$\begin{aligned}\psi &= tan^{-1}\left\{\frac{\mu_3\beta_2}{\mu_2\beta_3}\sqrt{\frac{{\beta_3}^2-c^2}{c^2-{\beta_2}^2}}\right\}\\ &= tan^{-1}\left\{\frac{\mu_3}{\mu_2}\sqrt{\frac{1-\frac{c^2}{{\beta_3}^2}}{\frac{c^2}{{\beta_2}^2}-1}}\right\}\lim_{\frac{\mu_3}{\mu_2}\to 0} \to 0,\pi,2\pi,...,etc.;\end{aligned}$$

Likewise, for Case 3 (equation 1.77)

$$\psi = cot^{-1}\left\{\frac{\mu_3}{\mu_2}\sqrt{\frac{1-\frac{c^2}{{\beta_3}^2}}{\frac{c^2}{{\beta_2}^2}-1}}\right\}\lim_{\frac{\mu_3}{\mu_2}\to 0} \to \pi/2,3\pi/2,...,etc.$$

The relationship between the frequency and the phase velocity for Case 2 (equation 1.74) becomes

$$tanh\frac{\omega f}{\beta_1}\sqrt{\frac{{\beta_1}^2}{c^2}-1}=\frac{\mu_2\beta_1}{\mu_1\beta_2}\sqrt{\frac{c^2-{\beta_2}^2}{{\beta_1}^2-c^2}}\,tan\left(\frac{\omega g}{\beta_2}\sqrt{\frac{c^2}{{\beta_2}^2}-1}\right) \tag{1.82}$$

Considering Case 3, equation (1.77) becomes

$$tan\frac{\omega f}{\beta_1}\sqrt{1-\frac{{\beta_1}^2}{c^2}}=\frac{\mu_2\beta_1}{\mu_1\beta_2}\sqrt{\frac{c^2-{\beta_2}^2}{c^2-{\beta_1}^2}}\,cot\left(\frac{\omega g}{\beta_2}\sqrt{\frac{c^2}{{\beta_2}^2}-1}-\frac{2n+1}{2}\pi\right) \tag{1.83}$$

where n indicates the mode of the response. If $\frac{\mu_3}{\mu_2}\to 0$,this may be written

$$tan\frac{\omega f}{\beta_1}\sqrt{1-\frac{{\beta_1}^2}{c^2}}=\frac{\mu_2\beta_1}{\mu_1\beta_2}\sqrt{\frac{c^2-{\beta_2}^2}{c^2-{\beta_1}^2}}\,tan\left(\frac{\omega g}{\beta_2}\sqrt{1-\frac{{\beta_2}^2}{c^2}}\right) \tag{1.84}$$

for the first mode. The negative square root has been taken. The result is similar to that expected from ray theory: the phase velocity at the free surface becomes large when the total reflected path is equal to one wavelength.

Clearly, $\frac{\omega f}{\beta_1}=0$ is a solution to (1.82) . However, if $\frac{\omega f}{\beta_1}$ is small but not zero we have(for $\psi = 0,\pi$, ...) from (1.82)

$$\frac{\omega f}{\beta_1}\sqrt{\frac{{\beta_1}^2}{c^2}-1}\lim_{\frac{\omega f}{\beta_1},\frac{\omega g}{\beta_2}\to 0}\to\frac{\mu_2\beta_1}{\mu_1\beta_2}\sqrt{\frac{c^2-{\beta_2}^2}{{\beta_1}^2-c^2}}\left(\frac{\omega g}{\beta_2}\sqrt{\frac{c^2}{{\beta_2}^2}-1}\right) \tag{1.85}$$

in which the terms in tanh and tan have been replaced by the first terms of their series expansions. If we make the substitution

$$x = \frac{\mu_2}{\mu_1}.\frac{{\beta_1}^2}{{\beta_2}^2}.\frac{g}{f} \tag{1.86}$$

we obtain from (1.85), on cross-multiplying and re-arranging,

$$\frac{c^2}{{\beta_1}^2} \underset{\frac{\omega f}{\beta_1} \to 0}{\lim} \to \frac{1 + \frac{{\beta_2}^2}{{\beta_1}^2}\, x}{1 + x} \tag{1.87}$$

Example 1.7

Consider the structure represented by the following parameters

$$\begin{array}{lll} \mu_1 = 25 & \mu_2 = 1 & \\ \beta_1 = 5 & \beta_2 = 1 & f = g \end{array}$$

Applying (1.87) it is found that $x = 1$, and $\frac{c}{\beta_1} \to 0.721$ as $\frac{\omega f}{\beta_1} \to 0$.

Considering further the vibration of the two layers as a composite plate ($\mu_3 << \mu_2$), it is necessary to investigate Case 3, represented by equation (1.83) when the measured phase velocity at the free surface becomes large. As $c \to \infty$, equation (1.84) yields

$$tan\frac{\omega f}{\beta_1} \underset{c \to \infty}{\lim} \to \frac{\mu_2 \beta_1}{\mu_1 \beta_2}\, .\, tan\frac{\omega g}{\beta_2} \tag{1.88}$$

Inserting the values of the parameters assumed for Example 1.7, equation (1.84) is true when $\frac{\omega f}{\beta_1} = 0.402, 0.969, ...,$ etc..

If the velocities of shear waves in media 1 and 2 can be determined in a two-layered composite free plate, equation (1.26) can be applied determine the ratio of the layer thicknesses, f/g.

Finally, $cot\ \psi$ in equation (1.78) can be rendered zero by another condition. This is the condition $c = \beta_3$. For the value of $\frac{c}{\beta_1}$ equal to $\frac{\beta_3}{\beta_1}$, therefore, points occur on the curves computed by means of equation (1.77) using the same values of $\mu_2, \mu_2, \beta_1, \beta_2, f/g$, assuming $\frac{\mu_3}{\mu_2}$ to be small. The curves obtained by putting $cot\ \psi = 0$ are the envelopes, representing the lower limits of the frequency, of the families of curves computed for various values of μ_3 and β_3, keeping $\mu_2, \mu_2, \beta_1, \beta_2$, and f/g fixed.

1.8 Approximate expressions. Cases 2 and 3.

Approximations to Cases 2 and 3

Some extreme and limiting cases have been considered. Relationships have been derived which may be of value in the approximate interpretation of experimental results. Approximations will be obtained, which are valid over limited ranges of the variables considered. Within these ranges, direct calculation is possible

and sufficient, and numerical methods are not required. Adequate plots can be obtained for approximate inverse solutions. This may be advantageous when interpreting experimental results.

Two approximations will be developed. (a) Case 2 (represented by Equation (1.24)) as $c \to \beta_2$, (b) Case 3 (represented by Equation (1.26)) as $c \to \beta_1$.

1.8.1 Case 2, $c \to \beta_2$

Consider equation (1.24), which relates the phase velocity at the free surface to the frequency of propagation of the waves. The structures are those designated by Case 2. If $c \to \beta_2$, the term in tanh must remain finite while the factor $\frac{\mu_2\beta_1}{\mu_1\beta_2}\sqrt{\frac{c^2-{\beta_2}^2}{{\beta_1}^2-c^2}}$ tends to zero.

Also, if $\frac{\mu_3}{\mu_2} \neq 0, tan\ \psi \to \infty$.

Therefore $\psi \to \frac{\pi}{2}, \frac{3\pi}{2}, ...,$ etc.

The term in tan in equation (1.24) must therefore tend to infinity. Therefore

$$\frac{\omega g}{\beta_2}\sqrt{1-\frac{{\beta_2}^2}{c^2}} - \frac{\pi}{2} \to \frac{\pi}{2}, \frac{3\pi}{2}, ..., \frac{2n+1}{2}\pi. \tag{1.89}$$

Denote $\frac{c-\beta_2}{\beta_1}$ by $\triangle\left(\frac{c}{\beta_1}\right)$, and we have

$$\frac{\omega g}{\beta_2}\sqrt{\frac{\beta_1}{\beta_2}.2\triangle\left(\frac{c}{\beta_1}\right)} \to \pi, 2\pi, ..., (n+1)\pi \tag{1.90}$$

$$\frac{\omega f}{\beta_1} \to \frac{f}{g}\left(\frac{\beta_2}{\beta_1}\right)^{\frac{3}{2}} [\pi, 2\pi, ..., (n+1)\pi] \Big/ \sqrt{2\triangle\left(\frac{c}{\beta_1}\right)} \tag{1.91}$$

where **n** is the node number.

If the layers are considered to vibrate as a composite plate, and the underlying medium is neglected, it is assumed that $\mu_3/\mu_2 \to 0$. We have, in equation (1.24), $\psi \to 0, \pi, 2\pi, ...,$ etc. and the result given in equation (1.91) becomes

$$\frac{\omega f}{\beta_1} \to \frac{f}{g}\left(\frac{\beta_2}{\beta_1}\right)^{\frac{3}{2}} \left[\frac{\pi}{2}, \frac{3\pi}{2}, ..., \frac{2(n+1)}{2}\pi\right] \Big/ \sqrt{2\triangle\left(\frac{c}{\beta_1}\right)} \tag{1.92}$$

Equations (1.91) and (1.92) are applied in the following example.

Example 1.8.1

The parameters used are as described in 1.8.5. Table 1.1 shows the results obtained by means of the approximate expressions (1.91) and (1.92), compared with those obtained by iteration using equations (1.74) and (1.24) respectively.

The results shown in Table 1.1 indicate that the accuracy obtainable by the approximations (1.91) and (1.92) improves as c approaches β_2, and is slightly better for mode zero than for mode one.

MODE	Structure 1 (Composite plate) For values of the parameters, see Example 1.7				Structure 2 (Two layers plus semi-inf.medium). For values values of the parameters, see Example 1.8.4			
	$\frac{\omega f}{\beta_1}\Big\rfloor_{\frac{c}{\beta_1}=0.21}$		$\frac{\omega f}{\beta_1}\Big\rfloor_{\frac{c}{\beta_1}=0.23}$		$\frac{\omega f}{\beta_1}\Big\rfloor_{\frac{c}{\beta_1}=0.21}$		$\frac{\omega f}{\beta_1}\Big\rfloor_{\frac{c}{\beta_1}=0.23}$	
	Exact Eqn. (1.74)	App. Eqn. (1.92)	Exact Eqn. (1.74)	App. Eqn. (1.92)	Exact Eqn. (1.24)	App. Eqn. (1.91)	Exact Eqn. (1.24)	App. Eqn. (1.91)
0	1.021	0.99	0.626	0.57	2.049	1.99	1.260	1.14
1	3.082	2.98	1.899	1.72	4.110	3.97	2.532	2.29

Table 1.1: Case 2. A comparison of the values obtained for $\frac{\omega f}{\beta_1}$ by means of the approximations (1.92) and (1.91) with those obtained by means of equations (1.74) and (1.77).

1.8.2 Case 3, $c \to \beta_1$

The alternate form of the expression (1.77) is as follows.

$$tan\frac{\omega f}{\beta_1}\sqrt{1-\frac{{\beta_1}^2}{c^2}} = \frac{\mu_2\beta_1}{\mu_1\beta_2}\sqrt{\frac{c^2-{\beta_2}^2}{c^2-{\beta_1}^2}}\,cot(\frac{\omega g}{\beta_2}\sqrt{1-\frac{{\beta_2}^2}{c^2}}+\psi) \tag{1.93}$$

In equation (1.93) as $c \to \beta_1$, we must have

$$tan\frac{\omega f}{\beta_1}\sqrt{1-\frac{{\beta_1}^2}{c^2}} \to 0, \tag{1.94}$$

and

$$cot(\frac{\omega g}{\beta_2}\sqrt{1-\frac{{\beta_2}^2}{c^2}}+\psi) \to 0, \tag{1.95}$$

where

$$cot\,\psi = \frac{\mu_3\beta_2}{\mu_2\beta_3}\sqrt{\frac{{\beta_3}^2-c^2}{c^2-{\beta_2}^2}}. \tag{1.96}$$

An approximation will be developed in which the trigonometrical functions are replaced by the initial terms of each series. We have from equation (1.93),

$$\frac{\omega f}{\beta_1}\sqrt{1-\frac{{\beta_1}^2}{c^2}} \simeq \frac{\mu_2\beta_1}{\mu_1\beta_2}\sqrt{\frac{1-\frac{{\beta_2}^2}{c^2}}{1-\frac{{\beta_1}^2}{c^2}}}\cdot\frac{1}{\frac{2n+1}{2}\pi-\frac{\omega g}{\beta_2}\sqrt{1-\frac{{\beta_2}^2}{c^2}}-\psi} \tag{1.97}$$

where n is an integer representing the mode of the response. Two cases will be considered. The first corresponds with the layers(media 1 and 2) vibrating

as a composite plate ($cot\,\psi \to 0$). The second corresponds with a structure in which the semi-infinite medium (medium 3) is rigid relative to the lower layer (medium 2), i.e $\mu_3 >> \mu_2$.

In the first case, $\psi \to \frac{\pi}{2}$, and the approximate expression (1.97) becomes

$$\frac{fg}{\beta_1\beta_2}\sqrt{1-\frac{{\beta_2}^2}{c^2}}\omega^2 - n\pi\frac{f}{\beta_1}\sqrt{1-\frac{{\beta_1}^2}{c^2}}.\omega + \frac{\mu_2\beta_1}{\mu_1\beta_2}\frac{\sqrt{1-\frac{{\beta_2}^2}{c^2}}}{1-\frac{{\beta_1}^2}{c^2}} \simeq 0. \tag{1.98}$$

In the second case, $cot\,\psi \to \frac{1}{\psi}$, and we have

$$\frac{fg}{\beta_1\beta_2}\sqrt{1-\frac{{\beta_2}^2}{c^2}}\omega^2 - \left[\frac{2n+1}{2}\pi - \frac{\mu_2\beta_3}{\mu_3\beta_2}\sqrt{\frac{1-\frac{{\beta_2}^2}{c^2}}{\frac{{\beta_3}^2}{c^2}-1}}\right]\frac{f}{\beta_1}.\omega + \frac{\mu_2\beta_1}{\mu_1\beta_2}\frac{\sqrt{1-\frac{{\beta_2}^2}{c^2}}}{1-\frac{{\beta_1}^2}{c^2}} \simeq 0. \tag{1.99}$$

where n represents the mode of the response.

Equations (1.107), (1.98) and (1.99) apply to ranges of phase velocity which are similar. However (1.98) and (1.99) are the better approximations.

1.8.3 Examples of Cases 2 and 3 as $c \to \beta_1$

Equations (1.24) and (1.26) represent the behaviour of the structures designated by cases 2 and 3. As $c \to \beta_1$, these equations can be simplified. At the limiting condition $c \to \beta_1$, the dimensionless frequency $\frac{\omega f}{\beta_1}$ can be written explicitly in terms of the phase velocity c at the free surface.

Case 2

The expression for Case 2 (equation 1.74) can be written in the form

$$tanh\frac{\omega f}{\beta_1}\sqrt{\frac{{\beta_1}^2}{c^2}-1} = \frac{\mu_2\beta_1}{\mu_1\beta_2}\sqrt{\frac{c^2-{\beta_2}^2}{{\beta_1}^2-c^2}}\,tan\left(\frac{\omega g}{\beta_2}\sqrt{1-\frac{{\beta_2}^2}{c^2}}-\psi\right) \tag{1.100}$$

where

$$tan\,\psi = \frac{\mu_3\beta_2}{\mu_2\beta_3}\sqrt{\frac{{\beta_3}^2-c^2}{c^2-{\beta_2}^2}}. \tag{1.101}$$

If $c \to \beta_1$, $tan(\frac{\omega g}{\beta_2}\sqrt{1-\frac{{\beta_2}^2}{c^2}}-\psi) \to 0, \pi, ..., n\pi$.

$$\frac{\omega g}{\beta_2} \simeq \frac{\psi}{\sqrt{1-\frac{{\beta_2}^2}{c^2}}}, \frac{\pi+\psi}{\sqrt{1-\frac{{\beta_2}^2}{c^2}}}, ..., \frac{n\pi+\psi}{\sqrt{1-\frac{{\beta_2}^2}{c^2}}} \tag{1.102}$$

where n is an integer representing the mode of the response. An expression for $\frac{\omega f}{\beta_1}$ is required. This is given by

$$\frac{\omega f}{\beta_1} \simeq \frac{\psi}{\sqrt{\frac{{\beta_1}^2}{{\beta_2}^2} - \frac{{\beta_1}^2}{c^2}}}\frac{f}{g}, \frac{\pi+\psi}{\sqrt{\frac{{\beta_1}^2}{{\beta_2}^2} - \frac{{\beta_1}^2}{c^2}}}\frac{f}{g}, ..., \frac{n\pi+\psi}{\sqrt{\frac{{\beta_1}^2}{{\beta_2}^2} - \frac{{\beta_1}^2}{c^2}}}\frac{f}{g}, \tag{1.103}$$

Case 3

Inserting the expression obtained for Case 3 (equation 1.77), we have

$$tan\frac{\omega f}{\beta_1}\sqrt{1-\frac{{\beta_1}^2}{c^2}} = \frac{\mu_2\beta_1}{\mu_1\beta_2}\sqrt{\frac{c^2-{\beta_2}^2}{c^2-{\beta_1}^2}}\, cot\left(\frac{\omega g}{\beta_2}\sqrt{1-\frac{{\beta_2}^2}{c^2}}+\psi\right) \tag{1.104}$$

where

$$cot\,\psi = \frac{\mu_3\beta_2}{\mu_2\beta_3}\sqrt{\frac{{\beta_3}^2-c^2}{c^2-{\beta_2}^2}}. \tag{1.105}$$

If $c \to \beta_1$, $cot\left(\frac{\omega g}{\beta_2}\sqrt{1-\frac{{\beta_2}^2}{c^2}}+\psi\right) \to 0.$

$$\frac{\omega g}{\beta_2} \simeq \frac{\frac{\pi}{2}-\psi}{\sqrt{1-\frac{c^2}{{\beta_2}^2}}}, \frac{\frac{3\pi}{2}-\psi}{\sqrt{1-\frac{c^2}{{\beta_2}^2}}}, ..., \frac{\frac{(2n+1)\pi}{2}-\psi}{\sqrt{1-\frac{c^2}{{\beta_2}^2}}} \tag{1.106}$$

where n is an integer representing the mode of the response. As before, we have also

$$\frac{\omega f}{\beta_1} \simeq \frac{\frac{\pi}{2}-\psi}{\sqrt{\frac{c^2}{{\beta_2}^2}-1}}\frac{f}{g}, \frac{\frac{3\pi}{2}-\psi}{\sqrt{\frac{c^2}{{\beta_2}^2}-1}}\frac{f}{g}, ..., \frac{\frac{(2n+1)\pi}{2}-\psi}{\sqrt{\frac{c^2}{{\beta_2}^2}-1}}\frac{f}{g} \tag{1.107}$$

Expressions (1.103) and (1.107) are both valid when $c = \beta_1$. At this point, both approximations should yield the same value of the dimensionless frequency, for a given set of parameters defining the structure. This is illustrated in Example 1.8.4.

1.8.4 Example 1.8.4

Consider the structure represented by the following parameters.

$$\begin{array}{llll} \mu_1 = 25\,, & \mu_2 = 1\,, & \mu_3 = 100 & \\ \beta_1 = 5\,, & \beta_2 = 1\,, & \beta_3 = 10\,, & f = g \end{array}$$

If $c = \beta_1$, the value of ψ in (1.103) is found to be 1.514 radians; in (1.107) the value is $(\frac{\pi}{2} - 1.514)$ radians. Both expressions yield the same value of $\frac{\omega f}{\beta_1}$. Table

1.2 shows the points obtained for the first nine modes. This result indicates that the curves representing the response of Case 2 touch those representing Case 3 at these points.

MODE	0	1	2	3	4	5	6	7	8
$\frac{\omega f}{\beta_1}$	0.31	0.95	1.59	2.23	2.87	3.52	4.15	4.80	5.43

Table 1.2: Cases 2 and 3. Values of $\frac{\omega f}{\beta_1}$ at which $c = \beta_1$ for the first nine modes

Equations (1.103) and (1.107) can also be used to determine the values of $\frac{\omega f}{\beta_1}$ if the layers (media 1 and 2) vibrate as a composite plate. Considering first equation (1.103) when $\mu_3 = 0$, $\psi = 0, \pi, ...,$ etc., we have

$$\frac{\omega f}{\beta_1} = 0, \frac{\pi}{\sqrt{24}}, ..., \frac{n\pi}{\sqrt{24}} \tag{1.108}$$

where n is an integer representing the mode of the response. In equation (1.107) when $\mu_3 = 0$ $\psi = \frac{\pi}{2}, \frac{3}{2}\pi, ...,$ etc., and the same values of $\frac{\omega f}{\beta_1}$ are obtained.

The values of $\frac{\omega f}{\beta_1}$ change rapidly over parts of the range for which expressions (1.103) and (1.107) are intended. The use of these equations may facilitate the interpretation of measurements.

1.8.5 Example 1.8.5

The accuracy obtained from expressions (1.103) and (1.107) can be shown by considering typical results. Values obtained by means of the approximate expression (1.103) are compared with those obtained by using equation (1.24). Two structures are considered. The first, a composite plate, is represented by the parameters assumed in Example 1.7. The second is the complete structure consisting of two layers overlying a semi-infinite medium; the parameters assumed in Example 1.8.4 are used.

The results of the computations are shown in Table 1.3. Case 2 only is considered. The results for Case 3 can be obtained by means of equations (1.107) and (1.26).

1.9 Approximation to Love system

Equation (1.58) yields the phase velocity implicitly as a function of the frequency. The system considered is the Love system, a single layer having a constant thickness overlying a semi-infinite medium. Equation (1.58) can be

MODE	Values of $\frac{\omega f}{\beta_1}$ when $\frac{c}{\beta_1} = 0.95$			
	Structure 1 (Composite plate) For values of the parameters, see Example 1.7		Structure 2 (Two layers plus semi-inf. medium). For values values of the parameters, see Example 1.8.4	
	Exact Eqn. (1.24)	Approximate Eqn. (1.103)	Exact Eqn. (1.24)	Approximate Eqn. (1.103)
0	0.000	0.00	0.349	0.31
1	0.718	0.64	1.058	0.95
2	1.414	1.28	1.742	1.59
3	2.089	1.92	2.409	2.23
4	2.750	2.57	3.067	2.88
5	3.405	3.21	3.719	3.52
6	4.054	3.85	4.368	4.16
7	4.702	4.50	5.014	4.81
8	5.347	5.14	5.659	5.45

Table 1.3: Case 2. A comparison of the values obtained for $\frac{\omega f}{\beta_1}$ by means of the approximation (1.103) with those obtained by means of equation (1.24).

approximated as follows, if the ratio of the Lame shear constants $\frac{\mu_2}{\mu_1} \to \infty$. We repeat the equation (1.58) for convenience.

$$tan\, s_1' f = \frac{\mu_2 s_2}{\mu_1 s_1'} \tag{1.109}$$

$$s_1{}^2 = \frac{\omega^2}{c^2} - \frac{\omega^2}{\beta_1{}^2}; \quad s_1'{}^2 = \frac{\omega^2}{\beta_1{}^2} - \frac{\omega^2}{c^2}; \tag{1.110}$$

Expanding the tangent term to the first power of its argument, we have

$$tan\, f\sqrt{\frac{\omega^2}{\beta_1{}^2} - \frac{\omega^2}{c^2}} \simeq \frac{\omega f}{\beta_1}\sqrt{1 - \frac{\beta_1{}^2}{c^2}} = \frac{\mu_2}{\mu_1}\frac{\beta_2}{\beta_1}\frac{\sqrt{1 - \frac{\beta_1{}^2}{c^2}}}{\sqrt{\frac{\beta_2{}^2}{c^2} - 1}} \tag{1.111}$$

Assume that the ratio of the Lame shear constants $\frac{\mu_2}{\mu_1} \to \infty$, and we have

$$\left(\frac{\omega f}{\beta_1}\right)^2 \left(1 - \frac{\beta_1{}^2}{c^2}\right) \simeq \frac{\pi^2}{4} \tag{1.112}$$

$$\frac{1}{c^2} \simeq \frac{1}{\beta_1{}^2} - \frac{\pi^2}{4}\frac{1}{\omega^2 f^2} \tag{1.113}$$

This expression provides an approximation to a Love system. The reciprocal of the square of the phase velocity of SH-waves is plotted against the reciprocal square of the frequency. The intercept on the axis of squared velocities is the reciprocal square of the velocity β_1. The slope of the plotted points yields the thickness of the surface layer f.

bibliog

Bibliography

[1] Ewing, W.M., W.S.Jardetzky and F.Press, Elastic waves in layered media. New York. McGraw-Hill. 1957. Equation (4-12), p. 210.

[2] Haskell, N.A., The dispersion of surface waves in multi-layered media. *Bulletin of the Seismological Society of America,* **43** (1). 1953, 17-34.

[3] Kurzeme, M., SH waves in layered pavement structures. Theoretical development and summary. *Preliminary Report A,,* The Institute of Highway and Traffic Research. The University of New South Wales. 1968. Equation (92).

[4] Love, A.E.H., Some problems in geodynamics. London. Cambridge University Press. 1911,1926.

[5] Nakano, H., Love waves in cylindrical co-ordinates. *The Geophysical Magazine,* **2**, 1930, 38-51.

[6] Officer, C.B., Normal mode propagation in three-layered liquid half space by ray theory. *Geophysics,* **16**, 1951, 207-212.

[7] Sato, Y., Study on surface waves, I. Velocity of Love waves. *Bulletin of the Earthquake Research Institute (Tokyo),* **29**, 1951, 1-11.

[8] Stoneley, R., Elastic waves at the surface of separation of two solids. *Proceedings of the Royal Society,* Series A, **106**, 1924, 416-428.

[9] Stoneley, R., The effect of a low-velocity internal stratum on surface elastic waves. *Monthly Notices of the Royal Astronomical Society: Geophysical Supplement,* **6**, 1950, 28-35.

[10] Su, S., and J.Dorman, The use of leaking modes in seismogram interpretation and in studies of crust-mantle structure. *Bulletin of the Seismological Society of America,* **55**, 1965, 989-1021.

[11] Thomson, W.T., Transmission of elastic waves through a stratified solid medium. *Journal of Applied Physics,* **21**, 1950, 89-93.

[12] Thrower, E.N., The computation of the dispesion of elastic waves in layered media, *Journal of Sound and Vibration,* **2**, 1965, 210-226.

[13] Tolstoy, I. and E.Usdin, Dispersive properties of stratified elastic and liquid media: a ray theory, *Geophysics,* **18**, 1953, 844-870.

Chapter 2

Computations

2.1 Introduction

Quantitative intepretation of experimental measurements is required. The structures which are considered are composed of two layers overlying a semi-infinite medium. Table 2.1 shows the possible permutations of the values of the shear wave velocities β_1, β_2 and β_3 within the structure. Corresponding with each permutation of shear wave velocities, one of the cases 1,2,3 or 4 is applicable. Table 2.1 shows the case which is applicable to a given range of phase velocities measured at the surface.

Programs have been written in Fortran in order to calculate the response expected. Listings of the programs follow. Sample data are supplied with each listing. The results are plotted in order to aid identification of the structures from the results of measurements.

The results are plotted in Figures 2.6.1 to 2.6.3. These figures show the phase velocity plotted against the frequency. Dimensionless units are used throughout. The frequency is expressed in units of $\frac{\omega f}{\beta_1}$. The phase velocity is expressed in units of $\frac{c}{\beta_1}$.

2.2 Case 1

```
c Horizontal shear waves. 2 layer. case 1A. june  1967 whc31p
c The velocity ratio must be greater than unity, and less than
c beta2/beta1, because E must be positive.

      dimension velrat(7),freq(7)
3     format(i1,f9.0,7f10.0)
4     format(7f3.2)
51    format(/7hc/beta1,3x7f6.3)
52    format(9hfrequency,1x7f6.3)                                    10
252   format(2f8.3)
```

Structure	Relative phase velocities of horizontally-polarized shear waves (SH waves)in the media composing the structure * Indicates that no real solution of Equation (1.20) exists.					
	$\beta_1 > \beta_2 > \beta_3$	$\beta_1 > \beta_3 > \beta_2$	$\beta_2 > \beta_3 > \beta_1$	$\beta_2 > \beta_1 > \beta_3$	$\beta_3 > \beta_1 > \beta_2$	$\beta_3 > \beta_2 > \beta_1$
REAL						
c > v1						
IMAG	s_1, s_2, s_3	s_1, s_2, s_3	s_1, s_2, s_3	s_1, s_2, s_3	s_1, s_2, s_3	s_1, s_2, s_3
CASE	*	*	*	*	*	*
v_1	β_1	β_1	β_2	β_2	β_3	β_3
REAL	s_1	s_1	s_2	s_2	s_3	s_3
v1 > c > v2						
IMAG	s_2, s_3	s_2, s_3	s_3, s_1	s_3, s_1	s_1, s_2	s_1, s_2
CASE	*	*	*	*	3	3
v_2	β_2	β_3	β_3	β_1	β_1	β_2
REAL	s_1, s_2	s_1, s_3	s_2, s_3	s_1, s_2	s_1, s_3	s_2, s_3
IMAG	s_3	s_2	s_1	s_3	s_2	s_1
CASE	*	2	1	*	2	1
v_3	β_3	β_2	β_1	β_3	β_2	β_1
REAL	s_1, s_2, s_3	s_1, s_2, s_3	s_1, s_2, s_3	s_1, s_2, s_3	s_1, s_2, s_3	s_1, s_2, s_3
v3 > c						
IMAG						
CASE	4	4	4	4	4	4

Table 2.1: Table showing applicable cases. The structures are classified by the relative velocities of shear waves in the component media. The cases are determined by the velocity of SH waves at the free surface of the structure.

```
 53     format(7hwave no,3x10f6.3)
 61     format(//4hcase, i3)
 62     format(4hmode2x3hf/g4x3hmu1,5x3hmu2,5x3hmu3,3x5hbeta1,3x5hbeta2
    +  ,3x5hbeta3)
 63     format(f3.0,f7.2,f6.0,5f8.0)
C  READ BRANCH,MODE,VALUES OF PARAMETERS
       WRITE(*,*) ' ENTER BRANCH,MODE,FOVERG,VALUES OF PARAMETERS '
       open(1,file='a:\case1.dat',status='old',form='formatted')
       open(5,file='a:\graph1.dat',status='unknown',form='formatted') 20
 11    READ(1,*)IBRNCH,XMODE,FOVERG,XMU1,XMU2,XMU3,BETA1,BETA2,BETA3
       write(*,*) ibrnch
       write(*,62)
       write(*,63)xmode,foverg,xmu1,xmu2,xmu3,beta1,beta2,beta3
 119   do 12 in=1,7
       velrat(in)=0
 12    freq(in)=0
       WRITE(*,*) ' ENTER SEVEN VALUES OF VELRAT '
       READ(1,*)VELRAT
       i=1                                                          30
```

```
      a=xmode*3.14159+1.
 20   cobta1=velrat(i)
      if(cobta1) 21,201,21
c       x=2 pi*g/lambda
 21   b=(xmu2*beta1/(xmu1*beta2))*sqrt(((beta2/beta1)**2-cobta1*cobta1)/
     +(cobta1*cobta1-1.))
      if(beta3) 212,212,211
 211  d=(beta3/beta1)**2-cobta1*cobta1
      f=sqrt(1.-cobta1*cobta1*((beta1/beta2)**2))
      e=(beta2/beta1)**2-cobta1*cobta1                                    40
      tnhpsi=(xmu3*beta2/(xmu2*beta3))*sqrt(d/e)
      psi=0.5*log((1.+tnhpsi)/(1.-tnhpsi))
      goto 213
c  establish a trial value of tan c, then interate until the values converge
 212  psi=0
 213  tanh1=exp(a)
      tanh2=exp(-a)
      xit2=b*(tanh1-tanh2)/(tanh1+tanh2)
 22   x=(a-psi)/f
c     write(*,*) ' 2 pi g /lambda = ', x                                  50
c     pause
      c=x*(sqrt(cobta1*cobta1-1.))*foverg
      xit1=sin(c)/cos(c)    ! trial value of tan c
c     test for  convergence
      if(xit1-xit2-0.001)101,199,102
 101  if(xit2-xit1-0.001)199,199,102
 102  xit2=(xit1+xit2)/2
      arg=xit2/b
      a=0.5*log((1.+arg)/(1.-arg))
      goto 22                                                             60
 199  freq(i)=cobta1*x*foverg
      i=i+1
      if(i-8)20,200,200
 200  write(*,51) velrat
      write(*,52) freq
      write(5,252) (-freq(i),velrat(i),i=1,7)
      goto 119       ! read further velocity data
 201  stop
      end
                                                                          70
```

Sample data for Case1.for is shown in Table 2.2.

1	0	1	1	16	4	1	4 2
1.97	1.35	1.3	1.25	1.2	1.15	1.1	
1.09	1.07	1.06	1.05	1.04	1.03	1.01	
0.0	0.0	0.0	0.0	0.0	0.0	0.0	

Table 2.2: Sample data for CASE1.FOR

2.3 Case 2

```
C       HORIZONTAL SHEAR WAVES 2 LAYER CASE 2 JUN 67 WHC31B
C       C MUST BE LESS THAN BETA1  AND GREATER THAN BETA2
        DIMENSION VELRAT(7),FREQ(7)
 3      FORMAT(I1,F9.0,7F10.0)
 4      FORMAT(7F3.3)
 51     FORMAT(2X/7HC/BETA1,3X7F6.3)
 52     FORMAT(1X9HFREQUENCY,1X7F6.3)
 252    FORMAT(2F8.3)
 53     FORMAT(1X7HWAVE NO,3X10F6.3)
 61     FORMAT(//4HCASE,I3)                                          10
 62   FORMAT(1X4HMODE2X3HF/G4X3HMU1,5X3HMU2,5X3HMU3,3X5HBETA1,3X5HBETA2
     +3X5HBETA3)
 63     FORMAT(F3.0,F7.2,F6.0,5F8.0)
C  READ BRANCH,MODE,VALUES OF PARAMETERS
        WRITE(*,*) ' ENTER BRANCH,MODE,FOVERG,VALUES OF PARAMETERS '
         open(1,file='a:\case2.dat',status='old',form='formatted')
        open(5,file='a:\graph2.dat',status='unknown',form='formatted')
 11     READ(1,*)IBRNCH,XMODE,FOVERG,XMU1,XMU2,XMU3,BETA1,BETA2,BETA3
        WRITE(*,*)IBRNCH
        WRITE(*,62)                                                 20
        WRITE(*,63) XMODE,FOVERG,XMU1,XMU2,XMU3,BETA1,BETA2,BETA3
 119    DO 12 IN=1,7
        VELRAT(IN)=0
 12     FREQ(IN)=0
        WRITE(*,*) ' ENTER SEVEN VALUES OF VELRAT '
        READ(1,*)VELRAT
        A=XMODE*3.14159+.7
        I=1
 20     COBTA1=VELRAT(I)
        IF(COBTA1)200,201,21                                        30
c       x= two pi g / lambda
 21    B=(XMU2*BETA1/(XMU1*BETA2))*SQRT((COBTA1*COBTA1-(BETA2/BETA1)**2)/
     +  (1.-COBTA1*COBTA1))
        IF(BETA3) 212,212,211
 211    D=(BETA3/BETA1)**2-COBTA1*COBTA1
        E=COBTA1*COBTA1-(BETA2/BETA1)**2
        PSI=ATAN((XMU3*BETA2/(XMU2*BETA3))*SQRT(D/E))
        GOTO 213
c establish a trial value of of tan c, then iterate until the values converge
 212    PSI=0                                                       40
```

```
213    XIT2=0
22     X=(A+PSI)/SQRT(COBTA1*COBTA1*((BETA1/BETA2)**2)-1.)
       C=X*(SQRT(1.-COBTA1*COBTA1))*FOVERG
       TANH1=EXP(C)
       TANH2=EXP(-C)
       XIT1=(TANH1-TANH2)/(TANH1+TANH2)   ! TRIAL VALUE OF TAN C
C      TEST FOR CONVERGENCE
       IF(XIT1-XIT2-0.001)101,199,102
101    IF(XIT2-XIT1-0.001) 199,199,102
102    XIT2=XIT1                                                    50
       A=ATAN(XIT2/B)+XMODE*3.14159
C THE PREVIOUS STATEMENT MAY NEED MODIFYING FOR MODES OTHER THAN ZERO ANL
       GOTO 22
199    FREQ(I)=COBTA1*X*FOVERG
       I=I+1
       IF(I-8)20,200,200
200    WRITE(*,51)VELRAT
       WRITE(*,52)FREQ
       WRITE(5,252) (FREQ(I),VELRAT(I),I=1,7)
       GOTO 119                                                     60
201    STOP
       END
```

Sample data for Case2.for iis shown in Table 2.3.

2	0	1	25	1	0	5	1	0
0.72111	0.67	0.62	0.55	0.5	0.4	0.3		
0.0	0.0	0.0	0.0	0.0	0.0	0.0		

Table 2.3: Sample data for CASE2.FOR

2.4 Case 3

```
C      HORIZONTAL SHEAR WAVES 2 LAYER CASE 3 JUN 67 WHC31C
C      C/BETA1   <VELRAT>   MUST BE GREATER THAN UNITY
       DIMENSION VELRAT(7),FREQ(7)
3      FORMAT(I1,F9.0,7F10.0)
4      FORMAT(7F3.2)
51     FORMAT(2X/7HC/BETA1,3X7F6.3)
52     FORMAT(1X9HFREQUENCY,1X7F6.3)
251    FORMAT(2F8.3)
53     FORMAT(1X7HWAVE NO,3X10F6.3)
61     FORMAT(//4HCASE,I3)                                          10
62   FORMAT(1X4HMODE2X3HF/G4X3HMU1,5X3HMU2,5X3HMU3,3X5HBETA1,3X5HBETA2,
    +3X5HBETA3)
63     FORMAT(F3.0,F7.2,F6.0,5F8.0)
C  READ BRANCH,MODE,VALUES OF PARAMETERS
```

```
      WRITE(*,*) ' ENTER BRANCH,MODE,FOVERG,VALUES OF PARAMETERS '
       open(1,file='a:\case3.dat',status='old',form='formatted')
       open(5,file='a:\graph3.dat',status='unknown',form='formatted')
11     READ(1,*)IBRNCH,XMODE,FOVERG,XMU1,XMU2,XMU3,BETA1,BETA2,BETA3
      WRITE(*,*)IBRNCH
      WRITE(*,62)                                                    20
      WRITE(*,63) XMODE,FOVERG,XMU1,XMU2,XMU3,BETA1,BETA2,BETA3
119    DO 12 IN=1,7
      VELRAT(IN)=0
12     FREQ(IN)=0
      WRITE(*,*) ' ENTER SEVEN VALUES OF VELRAT '
      READ(1,*)VELRAT
      A=XMODE*3.14159+1.
      I=1
20     COBTA1=VELRAT(I)
      IF(COBTA1)200,201,21                                           30
c      x= two pi g / lambda
21    B=(XMU2*BETA1/(XMU1*BETA2))*SQRT((COBTA1*COBTA1-(BETA2/BETA1)**2)/
     +  (COBTA1*COBTA1-1.))
      IF(BETA3) 212,212,211
211    D=(BETA3/BETA1)**2-COBTA1*COBTA1
      E=COBTA1*COBTA1-(BETA2/BETA1)**2
      PSI=1.5708-ATAN((XMU3*BETA2/(XMU2*BETA3))*SQRT(D/E))
      GOTO 213
c establish a trial value of of tan c, then iterate until the values converge
212    PSI=1.5708                                                     40
213    XIT2=0
22     X=(A-PSI)/SQRT(COBTA1*COBTA1*((BETA1/BETA2)**2)-1.)
      C=X*(SQRT(COBTA1*COBTA1-1.))*FOVERG
      XIT1=SIN(C)/COS(C)   ! TRIAL VALUE OF TAN C
C      TEST FOR CONVERGENCE
      IF(XIT1-XIT2-0.0001)101,199,102
101    IF(XIT2-XIT1-0.0001) 199,199,102
102    XIT2=XIT1
      A=XMODE*3.14159+1.570763-ATAN(XIT2/B)
      GOTO 22                                                        50
199    FREQ(I)=COBTA1*X*FOVERG
      I=I+1
      IF(I-8)20,200,200
200    WRITE(*,51)VELRAT
      WRITE(*,52)FREQ
      WRITE(5,251) (FREQ(I),VELRAT(I),I=1,7)
      GOTO 119
201    stop
      END
```

Sample data for Case3.for is shown in Table 2.4.

3	0	1	25	1	100	5	1	10
1.99995	1.97	1.90	1.8	1.75	1.72	1.70		
1.7	1.6	1.5	1.4	1.3	1.2	1.1		
0.0	.0.0	0.0	0.0	0.0	0.0	0.0		

Table 2.4: Sample data for CASE3.FOR

2.5 Case 4

```
c   horizontal shear waves. 2 layer. case 4 jun 1967 whc31d
c   c must be less than beta1, and less than beta2
      DIMENSION VELRAT(7),FREQ(7),ANG(7),XOUT(7)
 3    FORMAT(I1,F9.0,7F10.0)
 4    FORMAT(7F3.3)
 51   FORMAT(1X/'c/beta1',3x7F6.3)
 52   FORMAT(1X9Hfrequency,1x7F6.3)
 252  FORMAT(2F8.3)
 53   FORMAT(1X7Hwave no,3x10F6.3)
 54   FORMAT(1X3Harg,7x10F6.3)                                    10
 61   FORMAT(//4hcase,i3)
 62  FORMAT(4hmode3x3hF/G4X3Hmu1,5X3Hmu2,5X3Hmu3,3X5Hbeta1,3X5Hbeta1,3X
     +5Hbeta3)
 63   FORMAT(f3.0,f7.2,f6.0,5f8.0)
c  read branch,mode,values of parameters
      WRITE(*,*) ' ENTER BRANCH,MODE, VALUES OF PARAMETERS '
      open(1,file='a:\case4.dat',status='old',form='formatted')
      open(5,file='a:\graph4.dat',status='unknown',form='formatted')
 11   READ(1,*)IBRNCH,XMODE,FOVERG,XMU1,XMU2,XMU3,BETA1,BETA2,BETA3
      WRITE(*,*) IBRNCH                                           20
      WRITE(*,62)
      WRITE(*,63)XMODE,FOVERG,XMU1,XMU2,XMU3,BETA1,BETA2,BETA3
 119  DO 12 I=1,7
      VELRAT(I)=0.0
      XOUT(I)=0
      ANG(I)=0
 12   FREQ(I)=0
      WRITE(*,*) ' ENTER SEVEN VALUES OF VELRAT '
      READ(1,*) VELRAT
      A=XMODE*3.14159+1.                                          30
      I=1
 20   COBTA1=VELRAT(I)
      IF(COBTA1)201,201,21
c     x= two pi g / lambda
 21  B=(XMU2*BETA1/(XMU1*BETA2))*SQRT((1.-COBTA1*COBTA1)/((BETA2/BETA1)
     + **2-COBTA1*COBTA1))
      IF(BETA3) 212,212,211
 211  D=(BETA3/BETA1)**2-COBTA1*COBTA1
      E=(BETA2/BETA1)**2-COBTA1*COBTA1
      CTHPSI=(XMU3*BETA2/(XMU2*BETA3))*SQRT(D/E)                  40
```

```
      PSi=0.5*LOG((CTHPSI+1.)/(CTHPSI−1.))
      GOTO 213
c establish a trial value of of tanh c, then iterate until the values converge
212   PSI=0
213   COTH1=EXP(A)
      COTH2=EXP(−A)
      XIT2=B*(COTH1+COTH2)/(COTH1−COTH2)
22    X=(A+PSI)/SQRT(1.−COBTA1*COBTA1*((BETA1/BETA2)**2))
c     here psi is taken negative, otherwise no solution is possible.
c   it can be justified by taking the negative square root of d/e
      C=X*(SQRT(1.−COBTA1*COBTA1))*FOVERG
      TANH1=EXP(C)
      TANH2=EXP(−C)
      XIT1=(TANH1−TANH2)/(TANH1+TANH2)
      ANG(I)=A
C     WRITE(*,*) 'ANG = ',ANG
c     test for convergence
      IF(ABS(XIT1−XIT2) .LT. 0.001) GOTO 199
101   IF(XIT2−XIT1) 102,102,102
102   XIT2=(XIT1+XIT2)/2
C     WRITE(*,*) 'ARG = ',ARG
C     PAUSE
      ARG=XIT2/B
      A=0.5*LOG((ARG+1.)/(ARG−1.))
      GOTO 22
199   FREQ(i)=COBTA1*X*FOVERG
      XOUT(I)=X
      I=I+1
      IF(I−8)20,200,200
200   WRITE(*,51) VELRAT
      WRITE(*,52) FREQ
      WRITE(*,54) ANG
      WRITE(*,53) XOUT
      WRITE(5,252) (FREQ(I),VELRAT(I), I = 1,7)
      GOTO 119
201   STOP
      END
```

Sample data for Case4.for is shown in Table 2.5.

4	0	1	1	4	9	1	2	3
0.01	0.03	0.04	0.05	0.07	0.08	0.09		
0.1	0.2	0.3	0.4	0.5	0.6	0.7		
0.75	0.8	0.85	0.87	0.9	0.92	0.98		
0.0	0.0	0.0	0.0	0.0	0.0	0.0		

Table 2.5: Sample data for CASE4.FOR

2.6 Plotted results

The results obtained from the Fortran programs listed are shown in figures (2.6.1) to (2.6.3). The structures are represented by the values of shear moduli μ_1 to μ_3; μ_1 refers to the property of the surface layer, μ_2 refers to the property of the lower layer, and μ_3 refers to the property of the underlying semi-infinite medium. Thus the label 1 25 100 denotes $\mu_1 = 1, \mu_2 = 25, \mu_3 = 100$. The thicknesses of the layers are unity for both layers.

2.6.1 Case 1

Figure (2.6.1) shows the results obtained from a structure corresponding with Case 1. The results expected from two hypothetical structures are shown. The structures are designated by 1 25 4 and by 1 16 4. The first denotes a structure in which $\mu_1 = 1, \mu_2 = 25$ and $\mu_3 = 4$. The second denotes a structure in which $\mu_1 = 1, \mu_2 = 16$ and $\mu_3 = 4$. The thicknesses of the layers are unity for both layers.

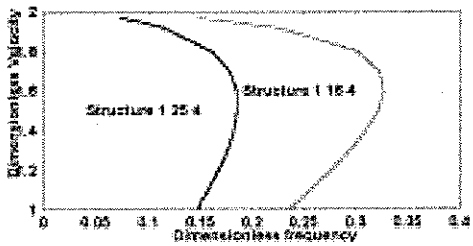

Figure 2.1: The results of calculations performed for some hypothetical structures. The phase velocity is shown plotted against the frequency, for structures of the type represented by Case 1.

2.6.2 Cases 2 and 3

Figure (2.6.2) shows the results obtained from a structure corresponding with Cases 2 and 3. The results expected from two hypothetical structures are shown. The structures are designated by 25 1 0 and by 25 1 100. The first denotes a structure in which $\mu_1 = 25, \mu_2 = 1$ and $\mu_3 = 0$. The second denotes a structure in which $\mu_1 = 25, \mu_2 = 1$ and $\mu_3 = 100$. The first structure corresponds with that of a compound free plate. The thicknesses of the layers are unity for both layers.

2.6.3 Case 4

Figure (2.6.3) shows the results obtained from a structure corresponding with Case 4. The results expected from two hypothetical structures are shown. The structures are designated by 1 4 25 and by 1 4 9. The first denotes a structure

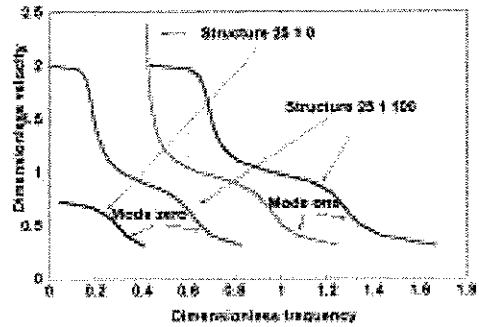

Figure 2.2: The results of calculations performed for some hypothetical structures. The phase velocity is shown plotted against the frequency, for structures of the type represented by Case 2 and Case 3.

in which $\mu_1 = 1, \mu_2 = 4$ and $\mu_3 = 25$. The second denotes a structure in which $\mu_1 = 1, \mu_2 = 4$ and $\mu_3 = 9$. The thicknesses of the layers are unity for both layers.

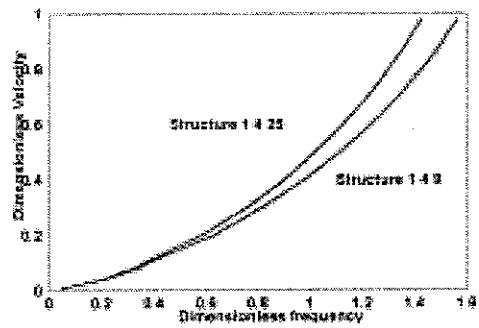

Figure 2.3: The results of calculations performed for some hypothetical structures. The phase velocity is shown plotted against the frequency, for structures of the type represented by Case 4.

Chapter 3

Experiments

This chapter includes some experimental results and their possible interpretations.

3.1 Case 1 - Model study

A piece of caneite, a synthetic material having texture similar to that of plastic foam, was placed on a laboratory bench. The thickness of the caneite was 0.11m. The velocity of SH waves was measured on the surface of the caneite. The results are shown in Figure (3.1). Numerical results of the measurements are given in the appendix.

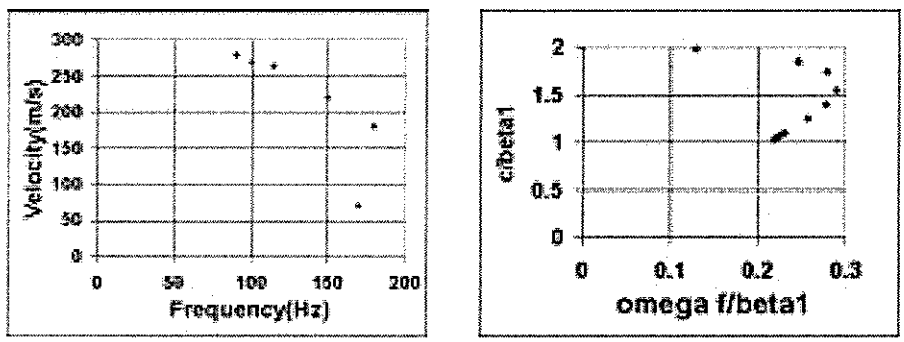

Figure 3.1: Case 1. SH waves on sample of caneite, 0.11m in thickness, resting on a laboratory bench.

The programme CASE1.FOR was used to attempt to match the experimental results to a hypothetical structure. The output obtained from the programme CASE1.FOR is shown plotted in Figure (3.1). This figure shows the dimensionless phase velocity c/β_1 plotted against the dimensionless frequency $\frac{\omega f}{\beta_1}$. The data file used to match the experimental results was as shown in Table 3.1.

After scaling the output of the programme CASE1.FOR, it is found that the theoretical structure consists of a surface layer 0.04m in thickness overlying a layer 0.045m in thickness. The total thickness of the two layers is 0.085m.

1 0 .9 1 16 4 1 4 2
1.97 1.85 1.75 1.55 1.4 1.25 1.1
1.09 1.08 1.07 1.06 1.05 1.04 1.03
0.0 0.0 0.0 0.0 0.0 0.0 0.0

Table 3.1: Sample of caneite. Datafile for CASE1.FOR

Laboratory Floor

The velocity of propagation of SH waves in the surface layer is 150m/sec. The velocity of propagation of SH waves in the underlying layer is 300 m/s.

3.2 Case 2. Laboratory floor

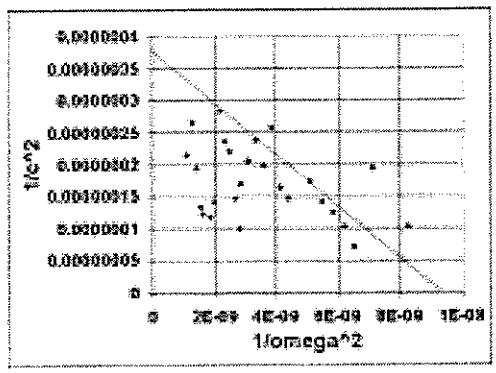

Figure 3.2: The results of measurements performed on a laboratory floor. The square of the reciprocal of the phase velocity is shown plotted against the square of the reciprocal of the angular frequency. The structure is of the type represented by Case 2.

Measurements were made on the floor of the Vehicle Laboratory, The University of New South Wales, Randwick, Australia. The results are shown in Figure (3.2). The estimated straight line represents the envelope of the points, corresponding with the lowest value of the argument of the tangent in equation (3.4). This is the condition under which Equation (3.4) is the most nearly true. The structure consists of bituminous concrete 0.21 metres in thickness, overlying damp sand 0.47 metres in thickness, overlying soft sand.

Numerical results of the measurements are given in the appendix.

From the approximate Equation (1.89) we have

$$\frac{\omega g}{\beta_2}\sqrt{1-\frac{{\beta_2}^2}{c^2}}-\frac{\pi}{2}\rightarrow\frac{\pi}{2},\frac{3\pi}{2},...,\frac{2n+1}{2}\pi. \tag{3.1}$$

The intercepts in Figure (3.2) are read as $1/c^2 = 3.75e-7$ and $1/\omega^2 = 9.2e-9$. The equation of the estimated trend is

$$\left(\frac{1}{c}\right)^2=\left(\frac{1}{1632}\right)^2-40.76\left(\frac{1}{\omega}\right)^2 \tag{3.2}$$

The thickness of the surface layer is f = 0.49 metres, calculated as $1/f^2 = 40.76/\pi^2$. The velocity of shear waves in the surface material is $\beta_2 = 1632$ m/s. Sand over Sandstone

3.3 Sand over sandstone

Measurements of the velocity of SH waves were made at the surface of a structure composed of sand overlying Sydney sandstone. The results are shown in Figure (3.3). In this figure, the phase velocity of SH waves at the surface of the structure is plotted against the wavelength. The results shown indicate that the velocity tends to limiting values at short and at long wavelengths. At short wavelengths, the velocity tends to the velocity of shear waves in the surface medium, the sand. At long wavelengths, the limit is the velocity of shear waves in the underlying medium, the sandstone. The continuous line shows the results calculated using LOVE.FOR using $\beta_1 = 31$ m/s, $\beta_2 = 335$ m/s, and thickness of layer = 0.27m .

Numerical results of the measurements are given in the appendix.

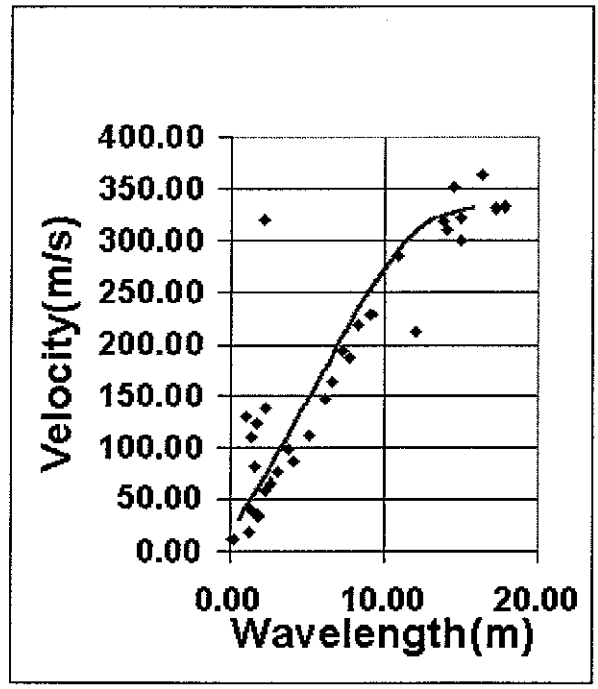

Figure 3.3: Results of measurements of SH waves at the surface of a structure composed of sand overlying sandstone. The measured thickness of the sand was 0.29 metres . The structure is of the type represented by Case 2.

The calculated line shown in Figure (3.3) was obtained with the aid of the following Fortran programme LOVE.FOR and the data file LOVE.DAT.

3.3.1 programme LOVE.FOR

```
c       Surface velocity of Love waves.
        dimension xlngth(40),vel(40),freq(40)
        open(1,file='a:\love.dat',status='old',form='formatted')
        open(5,file='a:\loveout.dat',status='unknown',form='formatted')
1        write(*,*) 'enter iva,ivb,h,x,c'
        read(1,*) iva,ivb,h,x,c
        m=1
15      va = iva
        vb=ivb
        xa=va ! initial value of <xa>                                    10
        write(*,*) 'va = ',va,'vb =',vb
        write(*,*) 'Depth upper layer =',h
        write(*,*) 'Ratio of shear moduli = ',x
10      xa=xa+c ! c is the increment in the phase velocity
        vx=xa
        if (vx - ivb) 11,11,100
11      z=(x*va/vb)*sqrt((vb*vb-vx*vx)/(vx*vx-va*va))
        wavln=((6.28*h/va)*sqrt(vx*vx-va*va))/atan(z)
        xlngth(m)=wavln
        vel(m) = vx                                                      20
        freq(m)=vx/wavln
        write(5,*)wavln,vx,vx/wavln
        xa=vx
50      continue
        goto 10
100     stop
        end
```

The data file is labelled LOVE.DAT; the results shown in Figure (3.3) were obtained with the following data file LOVE.DAT as input

31 335 0.27 150 10

3.4 Approximation to sand over sandstone

We seek an approximate solution which yields an estimate of the properties of the system. Rewriting equation (1.102) we have

$$\frac{\omega g}{\beta_2} \simeq \frac{\psi}{\sqrt{1-\frac{{\beta_2}^2}{c^2}}}, \frac{\pi+\psi}{\sqrt{1-\frac{{\beta_2}^2}{c^2}}}, ..., \frac{n\pi+\psi}{\sqrt{1-\frac{{\beta_2}^2}{c^2}}} \tag{3.3}$$

where n is an integer representing the mode of the response.

In equation (1.100), for Case 2, as $\mu_2 \to 0$, $\psi \to \frac{\pi}{2}$. We obtain the following approximation(see Equation (1.113))

$$\frac{1}{c^2} \simeq \frac{1}{{\beta_1}^2} - \frac{\pi^2}{4}\frac{1}{\omega^2 f^2} \tag{3.4}$$

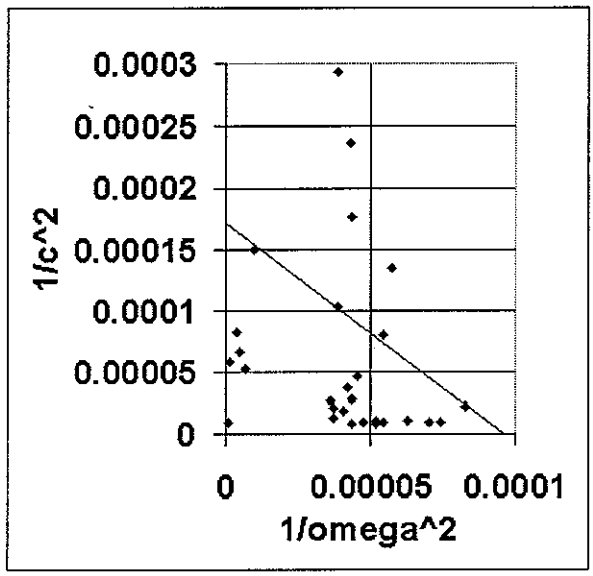

Figure 3.4: Results of measurements of SH waves at the surface of a structure composed of sand overlying sandstone. The measured thickness of the sand was 0.29 metres. The square of the reciprocal of the phase velocity is shown plotted against the square of the reciprocal of the angular frequency. The structure is of the type represented by Case 2.

We apply this approximation to the results shown in Figure (3.3). In Figure (3.4), the square of the reciprocal of the phase velocity is shown plotted against the square of the reciprocal of the angular frequency.

The plot of $1/c^2$ vs. $1/\omega^2$ in Figure (3.4) leads to

$$1/c^2 = 0.00017 - 1.7/\omega^2$$

$$f^2 = \pi^2/4\,(1/1.79)\,; f = 1.17m\ 1/{\beta_1}^2 = 0.00017$$

$\beta_1 = 77$ metres/sec.

The results shown in Figure (3.4) represent the measurements shown in Figure (3.3) at small values of $1/c^2$ and small values of ω^2. This was done in order to validate the approximation of the tangent of an argument by its argument. This result was not successful in estimating the thickness of the superficial layer.

The Equation (1.58) can be approximated for small values of the Lamé constant μ_2 in the underlying medium. If we set $\mu_2 = 0$, the result is [2]

$$\omega = \frac{c}{2f} \Big/ \sqrt{\left(\frac{c}{\beta_1}\right)^2 - 1} \tag{3.5}$$

An alternative form of the approximate Equation (3.4) can be derived from Equation (1.26). The result is as follows.

$$(2\pi)^2 \left(\frac{1}{\lambda}\right)^2 \simeq -\frac{1}{c^2}\omega^2 + \frac{\mu_2}{\mu_1 f} \tag{3.6}$$

Jones [3] derived and applied an analogous formula to the results of measurements of the velocity of Love waves.

3.5 Concrete slab resting on sand

It appears that the results of the measurements of the velocities of SH waves can be used to determine the interface depth of a simple layered structure. The results shown in Figure (3.5) were obtained on the surface of a concrete slab, 0.17 metres in thickness, resting on Botany Bay sand. The continuous line shows the expected result for a slab, 0.17m in thickness in which the velocity of shear waves $\beta_1 = 950m/s$. The approximate interpretation appears to be the more successful the greater the contrast in the shear moduli.

Numerical results of the measurements are given in the appendix.

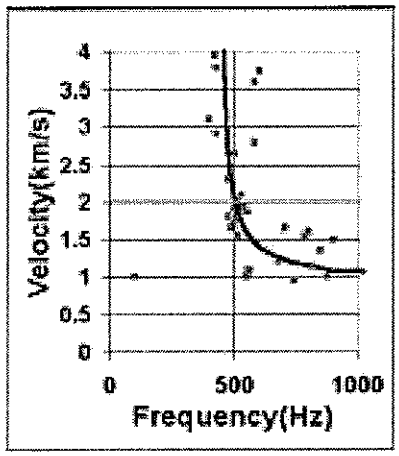

Figure 3.5: Results of measurements of SH waves at the surface of a structure composed a concrete slab resting on sand [4]. The structure is of the type represented by Case 2. The experimental points are shown. The continuous line is an approximation to the results of the measurements using Equation (3.5).

3.6 Case 3. Strip of pasteboard.

Measurements of SH waves were perfomed at the surface of a structure composed of a strip of pasteboard, 0.01m in thickness. The results of the measurements are shown in Figure 3.6. This figure shows the phase velocity of SH waves plotted against the frequency. The continuous line is an approximation to the results of the measurements using Equation 3.5, using as the velocity $\beta_1 = 950$m/s, and the thickness $f = 0.011$m.

Numerical results of the measurements are given in the appendix.

The points shown at frequencies less than 5khz may correspond with results to be expected for Case 3.

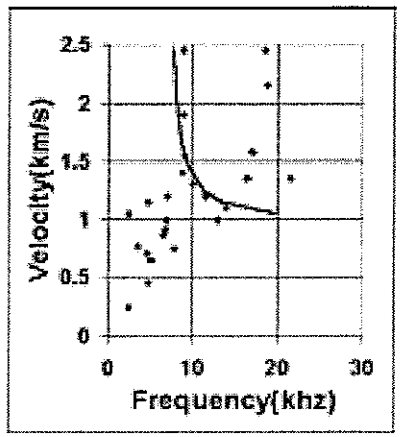

Figure 3.6: Results of measurements of SH waves at the surface of a structure composed of a strip of pasteboard, 0.01m in thickness. The structure is of the type represented by Cases 2 and 3. The experimental points are shown.

The form of the response includes that expected for Case 2. High velocities were observed at frequencies of 9khz and 18khz. These are assumed to correspond with values of $\frac{\omega f}{\beta_1}$ of 0.402 and 0.969 for modes 1 and 2 respectively, see Equation (1.84). If β_1 = 1000m/s, the thickness of the layer is given by 2*f and is approximately 0.012m.

The points shown at frequencies between 14khz and 17khz cannot be explained by the theory in its present form.

3.7 Case 4. Model study

A slab of caneite was placed on laboratory bench. The phase velocity of SH waves was measured at the surface of the slab. The results of the measurements are shown in Figure 3.7. This figure shows the phase velocity of SH waves plotted against the frequency. The slab of caneite was 0.025m in thickness, and the thickness of the underlying timber laboratory bench was 0.031m. Numerical results of the measurements are given in the appendix.

The programme CASE4.FOR was used in an attempt to determine the hypothetical structure which matches the experimental results. The output of the programme is shown plotted in Figure 3.7. This figure shows the phase velocity of SH waves plotted against the frequency. Both the quantities are in dimensionless units. The phase velocity is expressed as $\frac{c}{\beta_1}$, and the frequency is expressed as $\frac{\omega f}{\beta_1}$.

Using the results shown in Figure 3.7 the thickness of the slab was estimated as follows. The maximum value of $\frac{\omega f}{\beta_1}$ is 1.2. Thus $f = \frac{1.2 * 1800}{6000 * 2 * \pi} = 0.055m$. The total thickness of the structure is 0.055+0.055=0.11 m. This is in error by

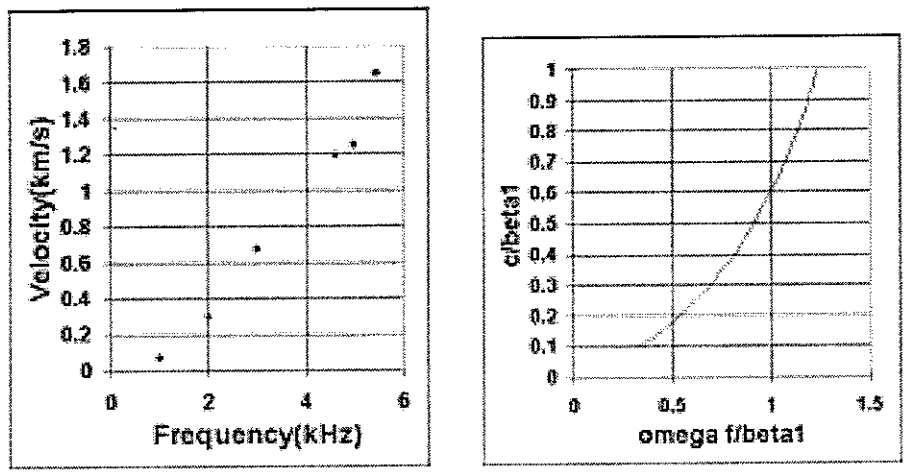

Figure 3.7: Case 1. SH waves on sample of caneite, 0.025m in thickness, resting on a laboratory bench.

a factor of approximately 2.

The data file used to match the experimental results was as shown in Table 3.2.

4 0 1 1 4 25 1 2 9
0.01 0.03 0.04 0.05 0.07 0.08 0.09
0.1 0.2 0.3 0.4 0.5 0.6 0.7
0.75 0.8 0.85 0.87 0.9 0.92 0.98
1.1 1.2 1.3 1.4 1.5 1.6 1.7
0.0 0.0 0.0 0.0 0.0 0.0 0.0

Table 3.2: Model study. Datafile for CASE4.FOR

The first-order approximation to the results given in Equation (1.80) is given by[1]

$$\frac{1}{c^2} \simeq \frac{1}{\beta_1^2} + \frac{1}{\omega^2 f^2} \tag{3.8}$$

3.8 Case 4. City street structure.

William Henry Street, Sydney

Measurements of the phase velocity of SH waves were performed on a roadway structure [5]. The structure consisted of 0.06m of asphaltic concrete, resting on 0.08m of bituminous macadam overlying clay. The results are shown in Figure (3.8). This figure shows the phase velocity plotted against the frequency of the

[1]The reasoning is as follows. $\frac{\omega f}{\beta_1}\sqrt{\frac{{\beta_1}^2}{c^2} - 1} \simeq -1$ i.e.

$$\frac{1}{c^2} \simeq \frac{1}{\beta_1^2} + \frac{1}{\omega^2 f^2} \tag{3.7}$$

wave. It also shows the square of the reciprocal of the phase velocity plotted against the reciprocal of the square of the angular frequency. Numerical results of the measurements are given in the appendix.

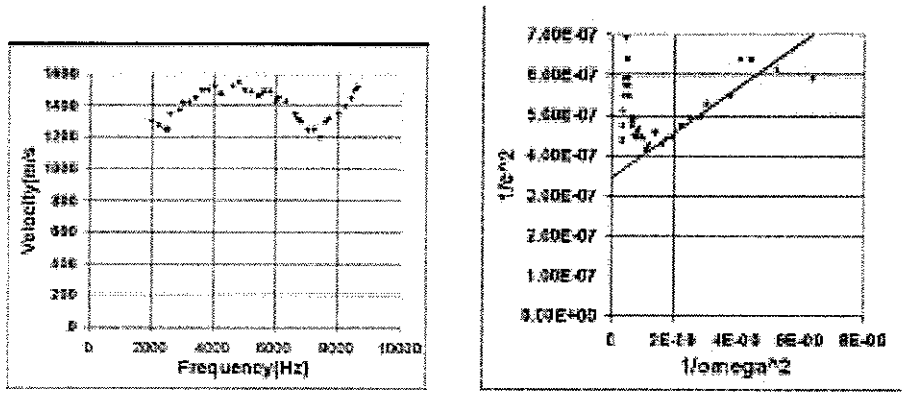

Figure 3.8: Case 4. SH waves on a roadway slab, consisting of 0.06m asphaltic concrete, overlying 0.08m bituminous macadam, overlying clay. William Henry Street, Sydney, Australia.

A first-order approximation is most nearly true at high values of the reciprocal of the square of the angular frequency. The approximate trend shown is expressed as

$$1/c^2 = 1/1690^2 + \frac{50.4}{\omega^2} \tag{3.9}$$

This approximation by Equation (3.8) yields a thickness of 0.13m, compared with a measured total thickness of 0.14m. The velocity of propagation of shear waves in the surface layer is 1690m/s.

3.9 Roadway structure. Case 4

Main Road 167

Measurements of the phase velocity of SH waves were performed on a roadway structure [6]. The structure consisted of 0.14m of asphaltic concrete, overlying 0.225m of compacted fine crushed rock, overlying sandy clay. The results are shown in Figure 3.9. This figure shows the phase velocity plotted against the frequency of the wave. It also shows the square of the reciprocal of the phase velocity plotted against the reciprocal of the square of the angular frequency.

Numerical results of the measurements are given in the appendix.

The approximate trend shown is expressed as

$$1/c^2 = 1/2890^2 + \frac{26}{\omega^2} \tag{3.10}$$

The approximation by Equation 3.8 yields a thickness of 0.20m, compared with a measured total thickness of 0.36m. The velocity of propagation of shear waves in the surface layer is 2890m/s.

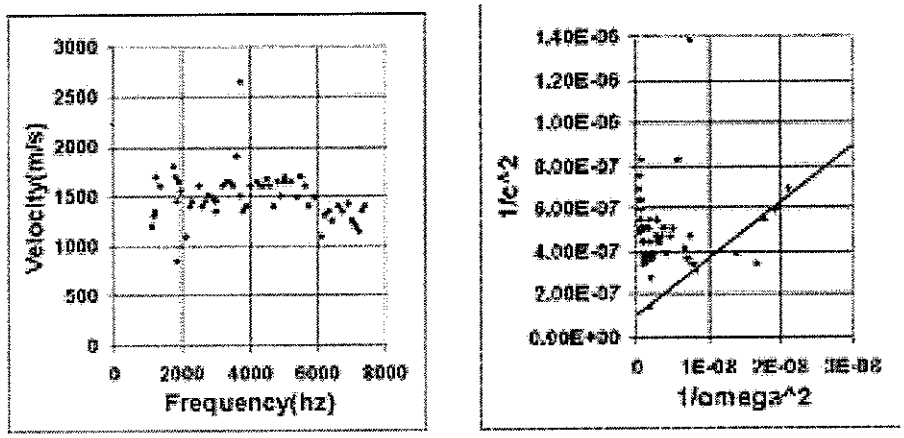

Figure 3.9: Case 4. SH waves on a roadway slab, consisting of 0.14m asphaltic concrete, overlying 0.225m of compacted fine crushed rock, overlying sandy clay. Main Road 167.

3.10 Pavement composed of asphaltic concrete, fine crushed rock and sandy clay

Copeland Street, Sydney

Measurements of the phase velocity of SH waves were performed on a roadway structure [7]. The structure consisted of 0.085m of asphaltic concrete, overlying 0.59m of compacted fine crushed rock, overlying sandy clay. The results are shown in Figure 3.10. This figure shows the phase velocity plotted against the frequency of the wave. It also shows the square of the reciprocal of the phase velocity plotted against the reciprocal of the square of the angular frequency.

Numerical results of the measurements are given in the appendix.

The effective double thickness of the surface layer is determined from the first of the two figures. SH waves are reflected from an interface purely as SH waves. If the surface velocity is high, the corresponding wavelength is equal to twice the thickness of the surface layer. In this case the observed high velocity occurs at 5600 Hz. The thickness is half of $\frac{1400m/s}{5600Hz} = 0.25m$. The deduced thickness of the surface layer is 0.12m, compared with the measured value of 8.5cm.

The plot of the reciprocal squares of the angular frequency and of the phase velocity appears not to yield useful information.

3.11 Conclusions

bibliog

Some experimental results have been presented, with possible interpretations.

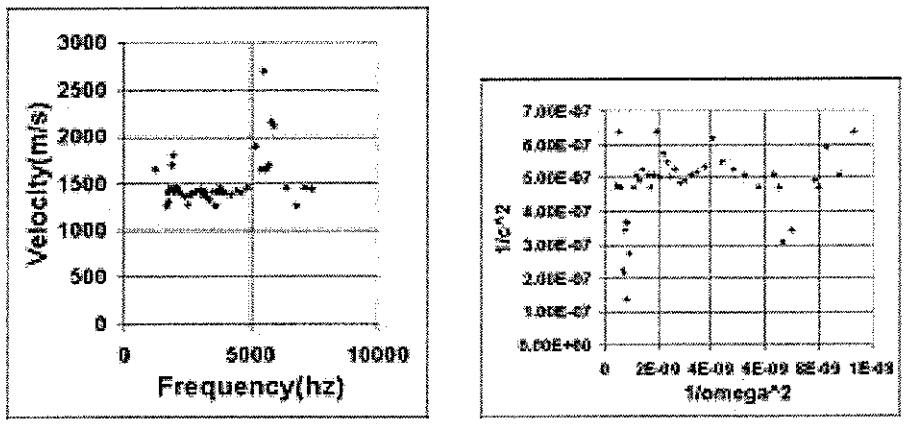

Figure 3.10: Case 4. SH waves on a roadway slab, consisting of 8.5cm asphaltic concrete, overlying 59cm of compacted fine crushed rock, overlying sandy clay. Copeland Street, Sydney, Australia.

Bibliography

[1] Cogill, W.H., Analytical methods applied to the results of the measurements of deflections and wave velocities at the fre surface of layered media. *Thesis,* The University of New South Wales. 1970.

[2] Ewing, W.M., W.S.Jardetzky and F.Press, Elastic waves in layered media. New York. McGraw-Hill. Equation (6-41), page 293.

[3] Jones, R., Measurement of dynamic properties of soil, *Geotechnique,* 8. 1958, 1-21. Equation (7), page 5

[4] Kurzeme, M., Field obsrvations of SH waves in layered pavements. *Report C, May 1969,* The Institute of Highway and Traffic Research. The University of New South Wales. 1969. Figure 8.

[5] *ibid.* Figure 17

[6] *ibid.* Figure 18

[7] *ibid.* Figure 19

Chapter 4

Appendix

4.1 Numerical results of the measurements.

This appendix contains the numerical results used to plot the figures shown in the body of the text. The results are presented in pairs of columns. The first column in each pair, $\frac{\omega}{2\pi}$ shows the frequency in herz. The second column in each pair shows the phase velocity c in metres per second.

$\frac{\omega}{2\pi}$	c	$\frac{\omega}{2\pi}$	c	$\frac{\omega}{2\pi}$	c	$\frac{\omega}{2\pi}$	c
90	280	100	270	115	265	150	220
180	180	170	70				

Table 4.1: Case 1 data. Model study Caneite 0.11m in thickness. Data plotted in Figure (3.1). CASE1.XLS

$\frac{\omega}{2\pi}$	c	$\frac{\omega}{2\pi}$	c	$\frac{\omega}{2\pi}$	c	$\frac{\omega}{2\pi}$	c
4797	2159	3544	2660	2763	2050	2151	2650
4488	1940	3407	1880	2660	2250	2083	2820
4227	2270	3289	2060	2566	1970	2019	3120
4049	2730	3177	2130	2476	2470	1971	3740
3969	2860	3071	2600	2401	2600	1887	2270
3814	3170	2967	2430	2294	1370	1752	3130
3677	2920	2863	2210	2224	2400		

Table 4.2: Case 2 data. Measurements on laboratory floor. Data plotted in Figure (3.2). VEHLAB.XLS

$\frac{\omega}{2\pi}$	c	$\frac{\omega}{2\pi}$	c	$\frac{\omega}{2\pi}$	c	$\frac{\omega}{2\pi}$	c
18.5	333	23.5	146	25.5	233	70	123
19	330	24	188	26	285	80	110
20	301	24	120	26	218	105	78
21	86	24	351	26.5	194	130	130
21.5	76	24.2	266	30	170	150	320
22	310	24.5	164	40	220		
22	362	25	229	50	82		
23	320	25.5	98	60	138		

Table 4.3: Case 2 data. Measurements on sand, 0.29m in thickness, resting on sandstone. Data plotted in Figure (3.3). 48MEDUSA.XLS

$\frac{\omega}{2\pi}$	c	$\frac{\omega}{2\pi}$	c	$\frac{\omega}{2\pi}$	c	$\frac{\omega}{2\pi}$	c
100	1000	500	2650	540	1950	700	1650
400	3100	500	1900	550	1850	740	950
425	3950	500	1700	550	1000	785	1550
430	3800	510	2000	560	1100	800	1600
430	2900	510	1780	580	3600	815	1150
480	2300	515	1550	580	2800	850	1350
480	1800	530	2100	600	3750	880	1000
490	1650	535	1930	680	1200	900	1500

Table 4.4: Concrete slab 0.17m in thickness resting on sand. Data plotted in Figure (3.5). data from Cogill [1] Thesis Fig. 8.6. FIG8_6.XLS

$\frac{\omega}{2\pi}$	c	$\frac{\omega}{2\pi}$	c	$\frac{\omega}{2\pi}$	c	$\frac{\omega}{2\pi}$	c
2500	250	6500	870	8950	1900	17000	1580
2500	1050	6700	920	9100	1550	18500	2450
3500	770	6900	1000	10000	1300	18800	2150
4850	450	7000	1200	11500	1200	21500	1350
4600	710	7800	750	13000	1000		
4800	1150	8800	1400	14000	1100		
5000	650	8900	2450	16500	1350		

Table 4.5: Strip of pasteboard, 0.01m in thickness. Data plotted in Figure (3.6). data from Cogill [1] Thesis Fig. 8.8. CASE3.XLS

$\frac{\omega}{2\pi}$	c	$\frac{\omega}{2\pi}$	c	$\frac{\omega}{2\pi}$	c	$\frac{\omega}{2\pi}$	c
1000	70	3000	680	5000	1250	5450	1650
2000	300	4600	1200				

Table 4.6: Strip of caneite, 0.025m in thickness, resting on a laboratory bench. Data plotted in Figure (3.7). data from Cogill [1] Thesis Fig. 8.9. CASE4.XLS

$\frac{\omega}{2\pi}$	c	$\frac{\omega}{2\pi}$	c	$\frac{\omega}{2\pi}$	c	$\frac{\omega}{2\pi}$	c
2000	1300	3800	1500	5600	1496	7400	1200
2200	1275	4000	1525	5800	1490	7600	1300
2400	1250	4200	1475	6000	1430	7700	1320
2500	1250	4250	1475	6100	1450	8000	1350
2600	1350	4600	1525	6300	1430	8200	1400
2900	1375	4800	1550	6600	1350	8400	1450
3000	1425	5000	1500	6700	1320	8500	1500
3200	1425	5200	1490	6800	1300	8600	1520
3400	1450	5400	1460	7000	1250		
3600	1500	5500	1470	7200	1250		

Table 4.7: William Henry Street, Sydney, Australia. Data plotted in Figure (3.8) Kurzeme [5] Fig. 17 data from MARCIS17.XLS

$\frac{\omega}{2\pi}$	c	$\frac{\omega}{2\pi}$	c	$\frac{\omega}{2\pi}$	c	$\frac{\omega}{2\pi}$	c
1100	1200	2600	1400	4010	1600	5600	1600
1150	1300	2700	1450	4200	1650	5700	1400
1200	1350	2800	1510	4300	1600	5900	1490
1230	1700	2900	1490	4400	1600	6100	1100
1350	1600	3000	1350	4500	1680	6200	1300
1750	1800	3010	1450	4600	1600	6300	1350
1800	1700	3200	1600	4700	1400	6400	1250
1900	1650	3300	1650	4800	1650	6600	1400
1950	1550	3400	1650	4900	1500	6700	1350
1850	1450	3500	1600	5010	1650	6900	1420
1850	850	3700	1500	5030	1650	7000	1250
2100	1100	3600	1900	5040	1700	7100	1200
2250	1400	3700	2650	5200	1650	7200	1150
2300	1450	3800	1350	5400	1490	7300	1350
2500	1600	3900	1400	5500	1700	7400	1400

Table 4.8: Main Road 167, Australia. Data plotted in Figure (3.9). Kurzeme [6] Fig. 18 data from MARCIS18.XLS

$\frac{\omega}{2\pi}$	c	$\frac{\omega}{2\pi}$	c	$\frac{\omega}{2\pi}$	c	$\frac{\omega}{2\pi}$	c
1200	1650	2200	1400	3300	1350	5200	1900
1650	1250	2300	1380	3400	1320	5400	1650
1700	1400	2400	1350	3500	1410	5500	2700
1750	1300	2500	1270	3600	1250	5600	1650
1780	1450	2600	1370	3700	1400	5700	1700
1800	1420	2700	1390	3800	1450	5800	2150
1900	1700	2800	1400	3900	1400	5900	2100
1950	1800	2900	1420	4200	1380	6400	1450
1970	1450	3000	1430	4400	1420	6800	1250
2000	1400	3100	1380	4600	1400	7100	1450
2100	1450	3200	1410	4800	1450	7400	1440

Table 4.9: Copeland Street, Sydney, Australia. Data plotted in Figure (3.10). Kurzeme [7] Fig. 19 data from MARCIS19.XLS

4.2 Variable Lamé constant μ

Situations may arise in which the Lamé constant μ varies with the depth.

Consider a system composed of a semi-infinite medium alone. We assume two-dimensional Cartesian co-ordinates, with z positive upwards. The Lamé constant μ is assumed to vary with the depth in the manner $\mu = \mu_0 - bz = \mu' - b(z+g)$.

$$\rho \frac{\partial^2 v}{\partial t^2} = \mu \nabla^2 v + \frac{\partial \mu}{\partial z} \frac{\partial v}{\partial z} \quad \text{Put } \sqrt{\mu} v = V \tag{4.1}$$

$$\frac{1}{\sqrt{\mu}} \rho \frac{\partial^2 V}{\partial t^2} = \frac{1}{\sqrt{\mu}} \frac{\partial^2 V}{\partial x^2} + \frac{1}{\sqrt{\mu}} \frac{\partial^2 V}{\partial z^2} - \frac{1}{\mu^{3/2}} \frac{\partial V}{\partial z} + \frac{1}{\mu^{5/2}} \frac{3}{4} V \tag{4.2}$$

This equation can be solved in terms of hypergeometric functions.